Science of the Total Environment 969 (2025) 178990

Contents lists available at ScienceDirect

Science of the Total Environment

journal homepage: www.elsevier.com/locate/scitotenv

Multiple asynchronous drought facets drive Mediterranean natural and cultivated ecosystems

Georgie Elias [a], Georgia Majdalani [a], Delphine Renard [a], Ghaleb Faour [b], Florent Mouillot [a,*]

[a] CEFE, Univ Montpellier, CNRS, EPHE, IRD, 1919 Route de Mende, CEDEX 5, 34293 Montpellier, France
[b] National Center for Remote Sensing, National Council for Scientific Research (CNRS), Riad al Soloh, Beirut 1107 2260, Lebanon

HIGHLIGHTS

- Drought is a multifaceted phenomenon, described by a comprehensive set of features
- Six yearly drought facets capture drought impact on major agro-environmental sectors under Mediterranean conditions
- Drought features are asynchronous, making it unlikely for all to be negative (minimal impact) or positive (harmful impact) across climatic years
- Six keystone features, each with functional significance, provide a synthetic drought impact assessment index

GRAPHICAL ABSTRACT

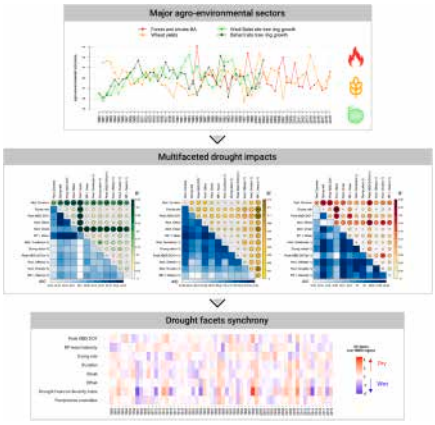

ARTICLE INFO

Editor: Fernando Pacheco

Keywords:
Multifaceted drought
DFEAT
Drought features
Agro-environmental threats
Synchrony

ABSTRACT

Drought is a keystone constraint with far-reaching implications for agro-environmental threats. Yet, drought indices are mostly hydro-meteorological or agricultural, obscuring evidence of the key role agro-ecosystem diversity plays in buffering the consequences of regional climatic variability. We then question how contrasted drought facets could differentially drive the functioning of agro-ecosystems, and whether the interannual asynchrony of these facets might prevent multi-crisis events. Here, we examine how a multifaceted characterization of yearly drought events differentially relates to key agro-environmental sectors and test how these drought facets synchronize over Lebanon, a Middle Eastern drought-prone country grappling with socio-economic and political crises. Using parsimonious multiple linear regression (MLR) models, we captured the combined functional roles of six yearly drought facets (duration, onset, offset, drying rate, peak drought day, and mean intensity of episodic rainfall pulses) on major agro-environmental sectors, including winter wheat yield, tree-ring radial growth, and area burned by wildfires. Delayed drought offset and faster spring soil moisture drying rates appeared more closely associated to increased burned areas ($R^2 = 0.25$), while drought onset and autumn rainfall pulses from the previous year were negatively linked to winter wheat yield ($R^2 = 0.12$), and tree radial growth switched from a control by drought onset and to duration with increasing altitude ($R^2 = 0.33$). The

* Corresponding author.
E-mail address: florent.mouillot@ird.fr (F. Mouillot).

https://doi.org/10.1016/j.scitotenv.2025.178990
Received 29 January 2025; Received in revised form 24 February 2025; Accepted 24 February 2025
Available online 1 March 2025

observed asynchrony in agro-environmental response to climate variability over the 1960–2020 period appears to buffer the occurrence of concomitant extremes, a pattern that we could relate to the asynchrony in their controlling drought facets. By demonstrating the functional role of each drought facet, we conclude on the efficiency of a compound functionally-sound drought facets index for synchronous agro-environmental climate crisis warning.

1. Introduction

Globally, an increasing frequency of natural hazards has been observed and documented over the last three decades, encompassing extreme weather events, such as heat waves, floods, wildfires, and droughts (Dixon et al., 2019; Krichen et al., 2023; Seneviratne et al., 2021). Drought, originating from an extended period of precipitation levels falling below the historical average for a particular region and timeframe, stands out as one of the most impactful hydro-climatic phenomena, affecting all aspects of society and environment (Wilhite and Pulwarty, 2017). Drought then represents a major disruptor of terrestrial ecosystem functioning, leading to significant agro-environmental threats (Hoover et al., 2020). These threats, defined as the negative impacts on the sustainability, productivity, and resilience of agricultural systems and their surrounding environments, occur irrespective of whether these systems are located in arid, semi-arid, or humid regions (Kmoch et al., 2024; Vicente-Serrano et al., 2020).

Drought is, however, a multi-disciplinary concept, typically classified into four types: meteorological drought (instigated by precipitation deficits), agricultural drought (often related to soil moisture depletion in the rooting zone), hydrological drought (water shortage in streams or storages), and socio-economic drought (imbalance between water supply and demand) (Haile et al., 2020; Wilhite and Glantz, 1985). These globally recognized categories capture, to a certain extent, the intricate nature of drought propagating through the entire hydrological cycle, with the assessment of each drought type relying on specific indices (Ndayiragije and Li, 2022). Although all drought indices are based on climatic variables, each index allows the quantification of different dimensions of drought in both time and space (Vicente-Serrano et al., 2012; Zargar et al., 2011). While certain indices rely on anomalies of a single climatic variable (such as precipitation or evapotranspiration) across different time scales, others, more complex, combine multiple soil hydrological processes (Seneviratne et al., 2021; Yihdego et al., 2019).

More recently, agricultural drought was extended to its ecological dimension to capture its impacts on the key functions of terrestrial ecosystems (Crausbay et al., 2017; Sadiqi et al., 2022; Vicente-Serrano et al., 2020). Some recent regional-to-global studies have identified robust relationships between the interannual variability of drought indices and key response variables in agro-ecosystems, such as tree-ring radial growth (Alfaro-Sánchez et al., 2018; Bhuyan et al., 2017; Gao et al., 2018; Gazol et al., 2017; Proutsos and Tigkas, 2020), forest growth and mortality (Allen et al., 2010, 2015; Choat et al., 2018; Lempereur et al., 2015), forest fires (Andrade and Bugalho, 2023; Barbero et al., 2019; Coscarelli et al., 2021; Lahaye et al., 2018; Turco et al., 2017; Vissio et al., 2023), and yield of major global crops (Leng and Hall, 2019; Lesk et al., 2016; Matiu et al., 2017; Peña-Gallardo et al., 2018; Santini et al., 2022). Each anomaly in agro-ecosystem functioning can lead to socio-ecologically-related agro-environmental threats, such as reduced wood production and carbon sequestration, forest and human infrastructure losses, or food insecurity, surpassing the response capacities of developing countries when happening concomitantly.

Some of these studies suggest that agro-environmental threats are multifactorial and respond to multiple facets of drought (Gao et al., 2018; Santini et al., 2022; Turco et al., 2017). Indeed, the interannual variability in climate variables can lead to contrasted agro-environmental responses, supporting the idea that the use of a single drought index (e.g., annual precipitation anomaly) might highly hide the complexity of drought impacts on natural and agro-ecosystems. Yet, most of these key findings about drought effects have relied on multi-scalar drought indices such as the Standardized Precipitation Index (SPI, McKee et al., 1993) and the Standardized Precipitation Evapotranspiration Index (SPEI, Vicente-Serrano et al., 2010). While both indices allow drought to be analyzed at multiple temporal scales, the minimum temporal window required for their calculation is one month. This restriction limits the temporal resolution of the analysis, omitting rainfall pulses and relying on local anomalies to a standard period hardly comparable between regions. There is, in turn, an increasing debate on drought characterization among ecologists (Slette et al., 2019), including limitations in the use of standardized precipitation index (Zang et al., 2020), associated with a lack of functional meaning of these meteorological or hydrological indices to ecological functions and processes. For instance, annual tree-ring increment has been widely assessed with seasonal precipitation and temperature while underlying processes of tree growth under water limitations respond to a soil water deficit threshold (drought onset) preventing cell turgor for elongation (Lempereur et al., 2015; Zribi et al., 2016). Ruffault et al. (2013) illustrated that, in the Mediterranean region, for a given regional climate and temporal trend, drought features such as onset, offset, and duration can produce contrasted local patterns.

These results thus questions how various agro-environmental threats might be linked to specific drought facets differentially responding to climate variability, and that some years might combine multiple extreme facet values as an integrated index for synchronous crisis. Differential drought features have been shown to affect socio-economic and environmental sectors in Europe (Blauhut et al., 2016), while Kukal and Irmak (2018) illustrate how co-occurring intra-sectorial impacts, as annual yields across crop types in the central US, differentially respond to a similar regional interannual climate variability and trend.

Here, we use the recently developed tool DFEAT (Drought FEature Assessment Tool) (Elias et al., 2024) to characterize yearly drought facets based on a daily generic soil water balance model over a hydrological year using the Keetch-Byram Drought Index (KBDI) (Keetch and Byram, 1968). Our aim is to i) test how each drought feature might differentially impact major agro-environmental functions and processes (wheat production, tree radial growth, and areas burned by wildfires) and ii) investigate the synchronies of these drought features anomalies as an integrated compound index for multi-agro-environmental crisis warning. We performed this analysis at the national level over Lebanon, a Middle Eastern country encompassing a gradient of summer-dry climates from Mediterranean-humid to arid, and recently under socio-political instability threatening food production (Kharroubi et al., 2021), ecosystems sustainability, and wildfire danger (Majdalani et al., 2022). More specifically, we seek to investigate which pairs of drought features (including drought onset, offset, duration, drying rate, peak drought day, and the mean intensity of rainfall pulses) exert a significant influence on key agro-environmental functions, and whether they synchronize or buffer each other across the 1960–2020 period. Our results will help to promote efficient national-level warning systems of concomitant drought-related agro-environmental threats that could worsen the socio-political instability of the country.

2. Materials and methods

2.1. Study area

The study area covers the national territory of Lebanon (10,452km^2),

a Mediterranean drought-prone country, located between 33°–35°N and 35°–37°E on the Eastern shore of the Mediterranean Sea (Fig. 1a). Even though Lebanon has limited geographic extent, yet it encompasses a diverse physiography, composed of two parallel mountainous chains 'Mount-Lebanon' and 'Anti-Lebanon' extending from southwest to northeast with an average altitude of 1400 m and 1050 m, respectively (Shaban, 2020). The highest point, Kornet el-Sawda, located in the western Mount-Lebanon range, reaches an elevation of 3088 m, the highest crest in the Middle-East region. Both mountainous chains are separated by the 'Bekaa Valley', where most of the country's agricultural lands are located (Jomaa et al., 2019; Lemenkova, 2022) (Fig. 1b). Among the main cultivated field crops, winter wheat and potatoes occupy the largest areas of the valley's cultivated arable lands (Nasrallah et al., 2019). In contrast, most of Lebanon's forests are aggregated over the 'Mount-Lebanon' mountain range. According to the most recent land use/cover type map of the country (LULC) (CNRS-L., 2019), the vegetation composed of forests, shrublands, and grasslands covers approximately 33.33 % (348,440 ha) of the Lebanese territory, including 87.8 % of forests and shrublands and 12.18 % of grasslands (Fig. 1c). Along the littoral zone and on the western slope of Mount-Lebanon, several coniferous (cedar, cypress, fir, juniper, and pine) and deciduous (carob tree, oaks, and pistachio tree) forests have developed (Hajar et al., 2010). Forest fires, which affect an average of 1500 ha of forests each year (Majdalani et al., 2022), pose a significant threat to the highly urbanized coastal zone interspersed with natural areas. The ecological significance of Lebanon's forests is rooted in the cultural value of *Cedrus libani*, the emblematic species of the country, which occupies a mere 0.86 % (1135 ha) of Lebanon's total forest cover. Additionally, these forests hold economic importance through wood production, which supports rural populations (Sattout et al., 2007).

Lebanon's diverse topography gives rise to a wide range of bioclimatic zones, largely driven by rainfall variability. Precipitation, which occurs predominantly between October and March, varies significantly across the country, from over 1000 mm annually in the northern coastal areas to <200 mm in the arid eastern regions (Jomaa et al., 2019). In particular, >95 % of the rainfall is concentrated in the winter months, particularly December and January. As a result of the unevenly distributed precipitation, Lebanon experiences a sharp climatological gradient, with relatively humid to sub-humid conditions along the coastal plains transitioning to arid conditions in the interior and eastern parts of the country (Haddad et al., 2014; Shaban et al., 2019). Lebanon's climate is also marked by prolonged warm and dry summers, extending from June to October, which lead to seasonal drought, with September typically being the driest month of the year (Kobrossi et al., 2021). The average annual temperature ranges between 14 °C in winter and 27 °C in summer in the coastal zone, with an average of 21 °C. In contrast, in the mountainous regions, the average annual temperature is below 12 °C (Shaban, 2020).

2.2. *Yearly drought features characterization from daily soil moisture time series*

For the multifaceted drought characterization, we relied on a previously developed automated tool, the Drought FEature Assessment Tool (DFEAT), to extract yearly drought features over a hydrological year (Elias et al., 2024). These features are derived from the Keetch-Byram Drought Index (KBDI; Keetch and Byram, 1968), representing the soil water deficit to field capacity (in mm), based on a simplified water-balance model simulating daily soil water loss (depletion) per day, and widely used in drought assessment studies (Andrade and Bugalho, 2023; Dimitrakopoulos and Bemmerzouk, 2003; Ganatsas et al., 2011; Nogueira et al., 2017). Despite it simple formulation, the KBDI index has been tested in diverse hydro-climatic regions, demonstrating a fair ability to replicate live fuel moisture content in certain Mediterranean shrub species (Dimitrakopoulos and Bemmerzouk, 2003; Ruffault et al., 2018). It has also shown a strong correlation with observed surface soil moisture under Mediterranean conditions (Ganatsas et al., 2011), and has been employed in agricultural research studies (Salehnia et al., 2018). Yet, Elias et al. (2024) acknowledged some limitations in the KBDI approach, which assumes an arbitrary soil depth and a type of soil. They also discussed the limitations of temperatures-based evapotranspiration estimates within the KBDI and similar drought indices.

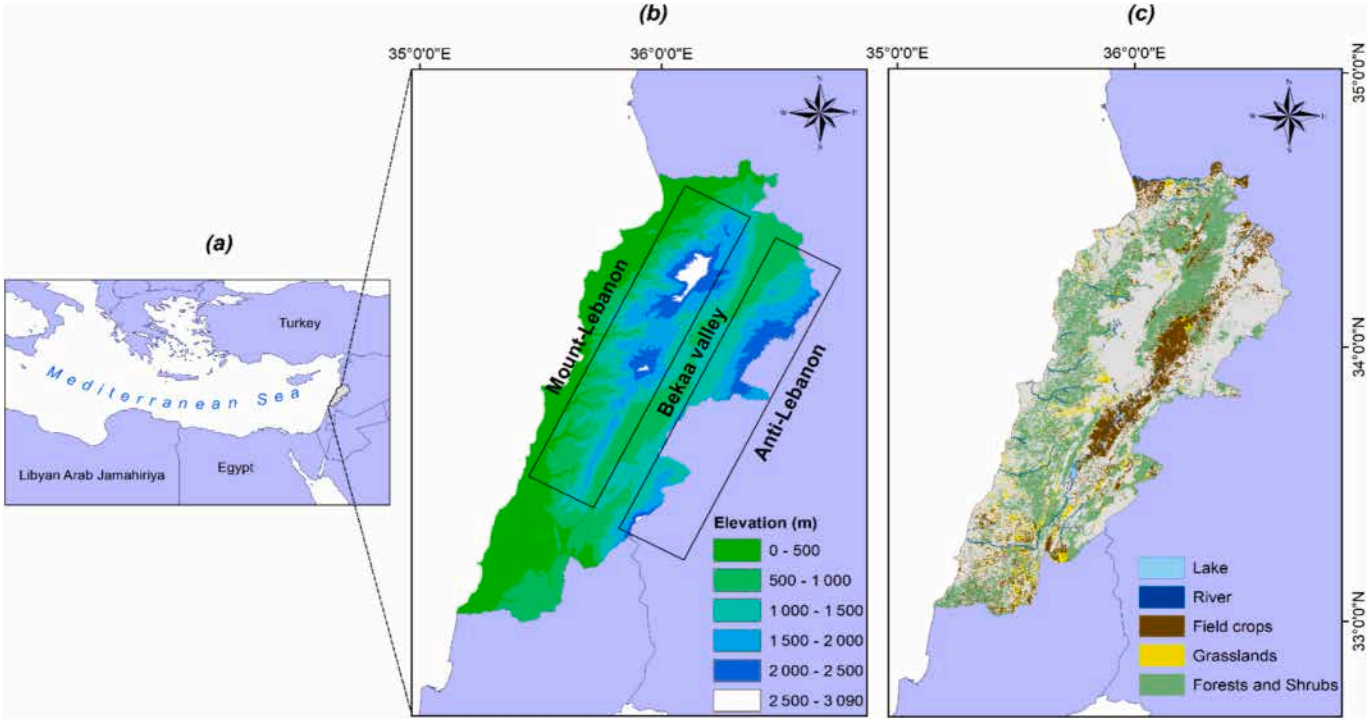

Fig. 1. (a) Location of Lebanon within the Mediterranean basin; (b) Digital Elevation Model (DEM) (adapted from ASTER GDEM Version 3) and major topographies; (c) Distribution of forests/shrublands, grasslands, field crops, rivers, and lakes (adapted from CNRS-L., 2019).

Accordingly, based on three soil desiccation thresholds (25 %, 50 %, and 75 % of the 200 mm field capacity, representing low, moderate, and extreme drought propagation levels, respectively) which were selected for their potential implications for agro-environmental threats, DFEAT extracts 19 yearly drought features related to the onset and offset timings, duration, severity, peak drought days, and the soil drying/rewetting rates (Elias et al., 2024). We considered the 25 % threshold (or KBDI-50) as an index of full soil profile refilling aiming at detecting multi-year drought without winter soil deep drainage, as a major information in ground water recharge (Reinecke et al., 2021). The 50 % (KBDI-100) and 75 % (KBDI-150) thresholds correspond to the maximum and minimum critical thresholds of plant water stress identified across biomes globally (Fu et al., 2024). Also, both thresholds affect vegetation functioning through stomatal closure and the subsequent plant transpiration and carbon assimilation (Granier et al., 1999), or tree growth through disruption of cell turgescence in Mediterranean forests (Lempereur et al., 2017). We proposed the two thresholds to cover various plant water use strategies (Klein, 2014) and soil texture (Saxton and Rawls, 2006). We acknowledge more drastic thresholds of 90 % might be of interest, but Elias et al. (2024) illustrated the high correlation between thresholds.

This tool has been recently applied and tested across Lebanon (Elias et al., 2024), using daily temperature and precipitation data from the open-source ERA5-Land climate dataset, downloaded at a 9 km spatial resolution (Muñoz-Sabater et al., 2021). This initial application of DFEAT over the Lebanese territory uncovered three different Mediterranean soil moisture dynamics or drought types: the Mediterranean typical dynamic (MED), the Humid mountainous Dynamic (HMED), and the Dry dynamic with multi-year drought occurrence (DRY-MED). These types were classified based on soil moisture desiccation patterns in relation to the country's climatic gradient.

In addition, preliminary analysis revealed inherent dependencies among many of the extracted drought features, which led to the final consideration of only six uncorrelated keystone features: drought duration for the moderate drought level, soil moisture drying rate, peak drought day occurrence, drought timings (onset and offset), and the mean intensity of rainfall pulses (Elias et al., 2024). Table 1 presents a brief definition of each of the six retained drought features. Together, these six features encapsulate the full development stages of drought events (Fig. 2). Accordingly, in this study, we have focused on these specific features due to their potential implications for understanding the multifaceted nature of drought and its threats to Lebanon's agro-environmental sectors.

Finally, we have combined these six drought features (DF) with a lagged version of each one-by-one year (DF *n-1*), acknowledging that eco-physiological processes of a given year can result from previous year's drought (Gao et al., 2018; Santini et al., 2022; Turco et al., 2017). We ended up with 12 drought features, six for each coincident drought year, and six for the lagged ones.

Table 1
Major drought features issued from DFEAT and their corresponding definitions and units (Elias et al., 2024).

Drought Features	Definition
Moderate Drought Duration	Number of days spanning between moderate drought onset and offset days of the year
Drying rate	Maximum daily soil water losses during drought development stage (mm/day)
Peak KBDI DOY	Day of the year (DOY) when KBDI reaches its peak severity value
Moderate Drought Offset	Day of the year (DOY) marking the end of the moderate drought level; when soil moisture is recovered to 50 % of its total available water content
Moderate Drought Onset	Day of the year (DOY) marking the onset of the moderate drought level; when soil lost 50 % of its total available water content
Rainfall pulses Mean Intensity	Mean intensity (in mm) of episodic rainfall pulses events occurring at the end of the dry season

2.3. Yearly information on agro-environmental threats

2.3.1. Winter wheat yield

Durum wheat, the strategic cereal crop of Lebanon (Abi Saab et al., 2019a; Nasrallah et al., 2018), was selected in our study to quantify the implications of interannual drought variability on key rainfed agricultural systems across the country. In Lebanon, wheat accounts for approximately 70 % of the total cultivated cereal area (45,000 ha), with around 30,000 ha of wheat fields out of the total cultivated land area of 223,000 ha, half of which are irrigated (Verner et al., 2018). Wheat yield is defined as the ratio of production over the harvested area. Annual wheat production (hectogram) and area (hectares) were obtained at the country level, from 1961 to 2019, from the Food and Agriculture Organization of the United Nations (FAO) (available at http://faostat.fao.org/default.aspx). The wheat calendar in Lebanon exhibits a well-defined sequence of phenological stages: sowing in October–November, germination and further growth through winter, flowering in spring (April–May), and grain filling (maturity) and harvest in June–July (Nasrallah et al., 2018, 2019). This timeframe enables a focused consideration of drought features that may directly impact winter wheat yield both during and in the lead-up to its growing season. Features that provide information outside the range of the growing season (from sowing to harvest) were not included in the analysis. This exclusion applies to drought duration, offset, Peak KBDI DOY, and coincident year rainfall pulses mean intensity, which correspond to the period after winter wheat harvest. The same applies to the lagged drought features (DF *n-1*), where only Peak KBDI DOY (*n-1*), drought offset (*n-1*), and rainfall pulses mean intensity (*n-1*) were considered, as they correspond to the period when the wheat is sown.

The presence of a unit root (i.e., presence of trend or seasonal pattern) on the wheat yield time series was tested, using the Augmented Dickey-Fuller test (ADF, Dickey and Fuller, 1979). Using this test, the null hypothesis could not be rejected, indicating that the wheat yield time series is not-stationary, and does not have a constant variance over time. This result could be attributed to advances in agricultural technology and improved management practices (Peña-Gallardo et al., 2019). Also, the serial correlation of wheat yields time series was analyzed based on their autocorrelation functions (ACF), which showed a significant autocorrelation for time lags of up to 15 years (Fig. 3a).

In order to remove bias introduced by non-climate factors and to account for autocorrelation in the wheat yield time series, we fitted an Autoregressive Integrated Moving Average function with structure (0,1,2) using the 'auto-arima' function from the 'forecast' R-cran package (Hyndman et al., 2020). The detrended wheat yields (Fig. 3.b) are considered in further analysis as more suitable indicator of the interannual variability in wheat production. Finally, to extract drought features over the area covered by the crop, we utilized the delineated field crops area derived from the LULC map (CNRS-L., 2019), which was resampled at 9 km resolution to match the spatial resolution of the climatic dataset used for this study (section 2.2).

2.3.2. Tree-ring data

To investigate the forest tree growth productivity response to drought features, we utilized six tree-ring chronologies encompassing the period 1960–2002, developed from six sites in Lebanon at six different altitudes (Touchan et al., 2005, 2014). Each chronology was constructed based on several trees, typically >10, of the same species growing in the same site. Five of the six tree-ring chronology sites belong to *Cedrus libani*, while one site belongs to *Abies cilicica*. Lebanon cedar (*Cedrus libani*) is a drought tolerant conifer of the *Pinaceae* family which is distributed along a wide altitudinal range (600–2300 m above sea level) in Turkey, Lebanon, and Syria (Güney et al., 2015), and is a protected species with high cultural value in Lebanon (Sattout et al., 2007). *Abies cilicica* is an endemic fir species native to the mountains of

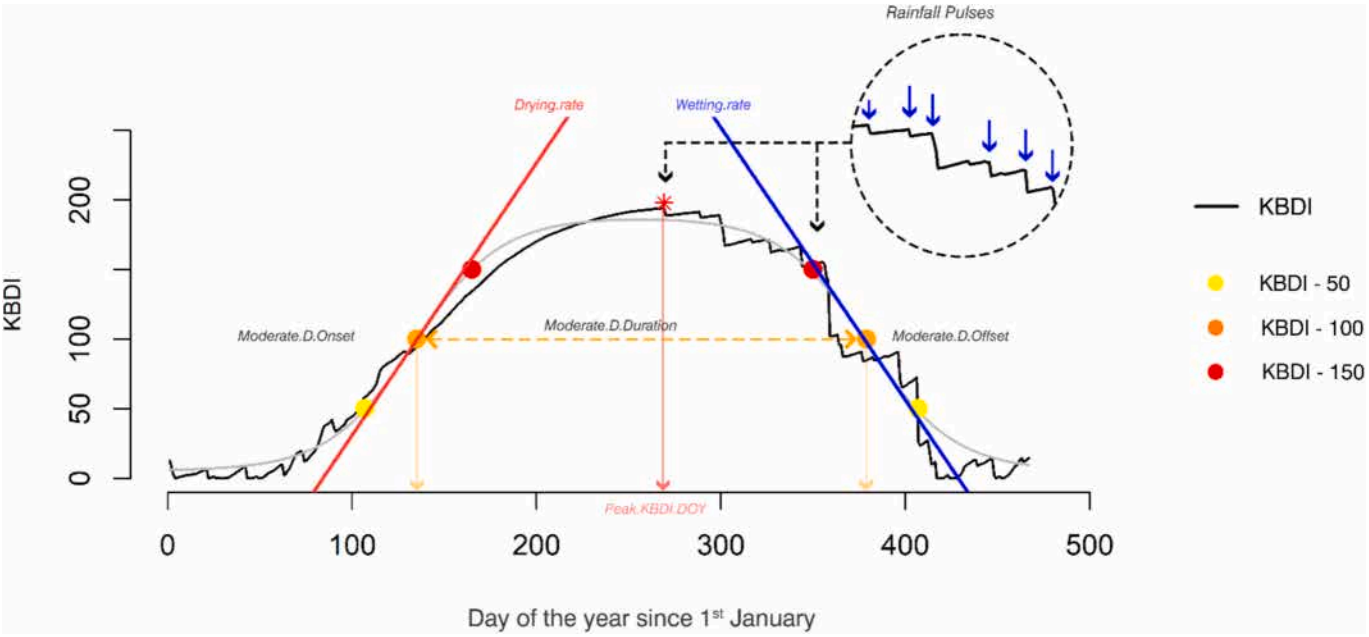

Fig. 2. The six retained drought features over Lebanon: Moderate Drought Duration (orange horizontal arrows), Drying Rate (red line), Peak KBDI DOY (red vertical arrow), Moderate Drought Offset (orange circle), Moderate Drought Onset (orange circle), and Rainfall Pulses Mean Intensity (small blue vertical flashes). KBDI time series (black line) and fitted seasonal dynamic (light grey line) are represented.

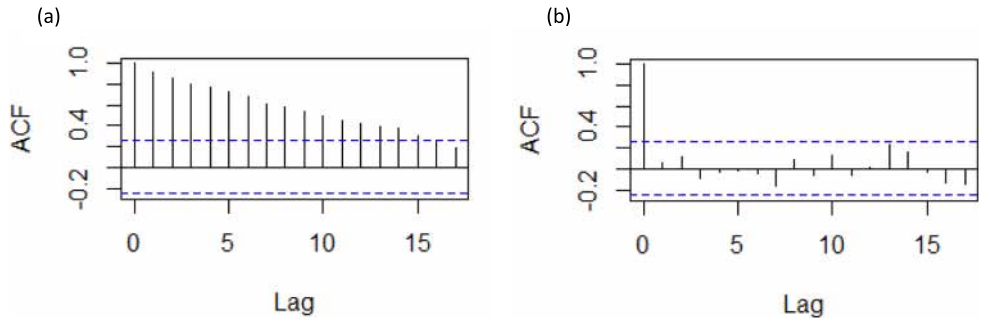

Fig. 3. (a) Autocorrelation Function (ACF) diagrams for the wheat yields time series for the period 1961–2019; (b) Autocorrelation Function (ACF) diagrams of residuals from the ARIMA (0,1,2). Blue dashed lines indicate the 95 % confidence intervals.

the Eastern Mediterranean region. It is found in three primary distribution areas in Turkey, Syria, and Lebanon (Mount-Lebanon Range) (Beridze et al., 2021). The species is at risk in its lower elevation habitats due to the aridization of local climates (Aussenac, 2002) and is classified as a near-threatened species in Lebanon where fir forests mark their southernmost geographic range (Awad et al., 2014).

The tree-ring data was downloaded from the International Tree-Ring Data Bank (ITRDB), (accessed online at http://www.ncdc.noaa.gov/paleo/treering.html). The processing of tree-ring width measurements and the full methodology are detailed in Touchan et al. (2005). The national distribution of these different sites offers the opportunity to study drought features impacts on tree-ring width growth following an altitudinal aridity and temperature gradient. Table 2 presents additional information on each site.

2.3.3. Forest and Shrubland burned areas

As a major environmental threat, we used the annual wildland burned area data obtained from remotely sensed data over Lebanon from Majdalani et al. (2022). The fire data cover the 1984–2019 period, including 2302 fires burning an estimated total area of 53,306 ha, with a mean yearly value of 1500 ha burned/year in Lebanon (Fig. 4a). The fire season extends over a protracted period, ranging from June to November (Majdalani et al., 2022).

Table 2
Site information for tree-ring width chronologies, including site name, the dominant tree species at the study sites, the elevation above sea level, latitude, and longitude.

Site Name	Species	Elevation (m)	Latitude (°)	Longitude (°)
Wadi Balat	*Abies cilicica*	1170	34.47	36.23
Herch Ehden	*Cedrus libani*	1640	34.3	35.98
Bsharri	*Cedrus libani*	1940	34.23	36.03
Arz Jaj	*Cedrus libani*	1780	34.13	35.82
Barouk	*Cedrus libani*	1775	34.68	35.68
Maaser Al Shouf	*Cedrus libani*	1700	33.67	35.69

The Burned Area (BA) time series was checked for trend stationarity using the KPSS test (Kwiatkowski et al., 1992), which did not provide sufficient evidence to reject the null hypothesis, indicating that the BA time series is trend stationary (Fig. 4b). However, marked year-to-year oscillations are present in the BA time series. First, we normalized the positively skewed BA by applying a logarithmic transformation ($y = \log10\ (BA)$) for the normality requirement, as verified by the Shapiro-Wilk test. Then, the time series of log10 (BA) was further detrended to minimize the influence of slowly changing factors such as the gradual

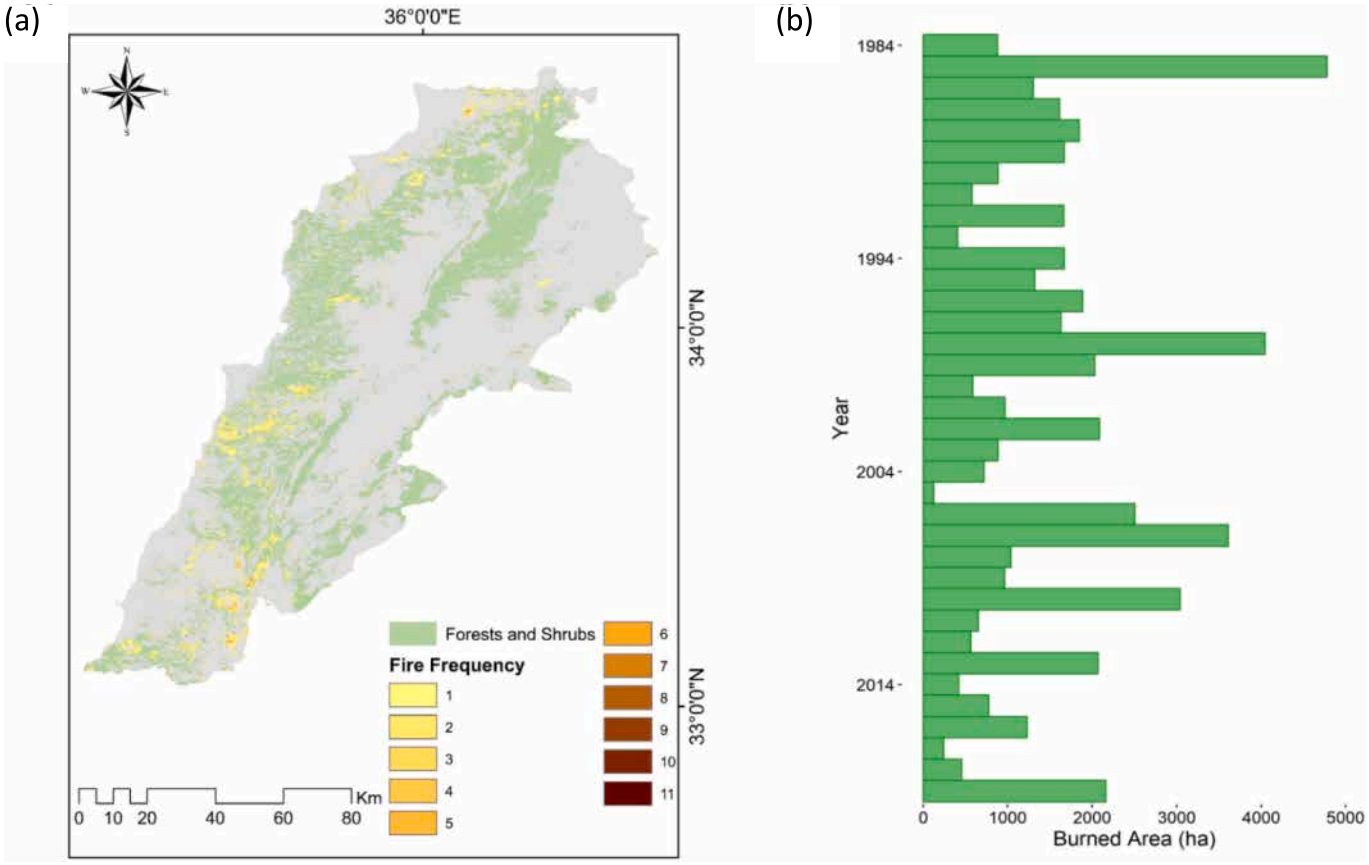

Fig. 4. (a) Fire frequency map, and (b) yearly burned area (ha) over the forest and shrub cover in Lebanon (1984–2019) (adapted from Majdalani et al., 2022).

increase in fire management and land-use changes, following similar approaches used in modeling drought-fire relationships. Finally, the fire occurrence map was resampled at 9 km spatial resolution to match the spatial resolution of the climatic dataset used for this study (section 2.2) and extract climate variables over each pixel burned at least once.

2.4. Statistical analyses

To perform correlations between pixel-level drought features and national-level agro-environmental information, the weighted mean of drought features was calculated for wheat fields and burned areas, with relative weights being the surface of each land cover in each 9 km climate pixel over Lebanon. For tree-ring chronologies, a pixel-based evaluation was conducted, as the data on tree-ring width measurements is available for six specific locations precisely located by their latitude and longitude coordinates.

To estimate the impacts of coincident drought features (current summer drought conditions) and their lagged values by one year (antecedent drought conditions) on the previously mentioned key agro-environmental variables, we performed a Multiple Linear Regression model (MLR), an empirical method widely used in drought impact assessment studies (Belhadj-Khedher et al., 2020; Bhuyan et al., 2017; Bouras et al., 2021; Turco et al., 2017; Vissio et al., 2023). This data-driven statistical method links yearly values of burned areas, wheat yields, and tree radial growth taken as dependent variables with the selected drought features (independent or predictor variables) (Eq. 1):

$$Y = \beta_0 + \beta_1 X_1 + \beta_2 X_2 + \beta_n X_n + \varepsilon \quad (1)$$

where Y is the predicted value of the dependent variables, β_0 is the y-intercept when all the independent variables are zero, β_1 and β_2 are the regression coefficients that represent the sensitivities of Y to the independent variables X_1 and X_2 presented here by the six retained drought features. ε is a stochastic noise term that captures all other (neglected) factors that influence the dependent variables (Y) other than X_1 and X_2 (Tranmer and Elliot, 2008).

We limited our analysis to test the importance of all possible combinations for only two explanatory variables (pairs of drought features). Accordingly, we fitted all possible models (i.e., in-sample models) with the combination of two selected predictors at each time (2 predictors out of 12) aiming to identify the maximum correlation values among all the models evaluated. The goodness of fit of the developed models was estimated using the coefficient of determination (R^2) as an indication of the explained variance and was considered statistically significant for p-values <0.05. Additionally, to identify the best statistically significant models, we computed the minimum Akaike information criterion (AIC) value among all the developed models (Akaike, 1974), using the 'performance' R-cran package, providing utilities for computing measures to evaluate models quality and fit (Lüdecke et al., 2021). The AIC measures the goodness of a statistical model based on a trade-off between its accuracy (that is, the explained variance) and its complexity (that is, the number of free parameters). Following this criterion, the model with the lowest AIC is preferred. The retained models presented and discussed in Sections 3 and 4 where those residuals satisfy the hypothesis of normality, zero autocorrelation, and constant variance (i.e., homoscedasticity tested using the Breusch-Pagan test, using the 'bptest' function from the 'lmtest' R-cran package) (Schmidt and Finan, 2018; Verran and Ferketich, 1987; Zeileis and Hothorn, 2002).

To get a more nuanced understanding into the uncertainty surrounding the coefficient estimates (regression model slopes) and R^2 values of our retained significant models, we leveraged a bootstrap resampling technique. This approach utilizes the "pairs (random x)" method, which resamples pairs of observations (encompassing both the dependent and all independent variables) from the original dataset for

each model, with replacement (Davison and Hinkley, 1997). This iterative process is repeated over 1000 replicates, generating bootstrap samples that faithfully replicate the dependence structure within the variables, and was implemented using the "boot" R-cran package (Canty and Ripley, 2017). Subsequently, the model is refitted on these resampled datasets. By treating the observed data as a singular realization of the underlying process, our bootstrap approach enables us to construct numerous hypothetical replications of the same process.

The results are presented in regression plots using the 'Corrplot' R-cran package (Wei et al., 2021), wherein the upper half of the plots, the circle color and size represent the strength of multiple R^2 values for each constructed model, reflecting the correlation between two independent variables (X1 from rows and X2 from columns) in relation to the targeted agro-environmental variables. The diagonal line in the upper half represents the correlation between a single independent variable (drought feature) and the targeted agro-environmental variables. Asterisks indicate significant *p*-value levels: * < 0.05, ** < 0.01, *** < 0.001. In the lower half of the plots, the numeric values represent the Akaike Information Criterion (AIC).

Heat maps were produced to illustrate synchronicity phases between the six selected drought features using the 'ggplot2' package in R (Wickham et al., 2016).

All the statistical analyses were performed in R 4.3.1 statistical environment (Core Team, 2021).

3. Results

3.1. Burned area / drought assessment

To identify the key drought features potentially affecting the inter-annual BA variability in Lebanon, we created a regression plot presenting all potential explained variances (R^2) and AIC values between the detrended log10 (BA) and the combination of different drought features pairs (Fig. 5). Since both the dependent and independent variables are in standardized forms, the model's slope coefficient values indicate the extent of change in standard deviations.

The overall examination of the constructed Drought-BA regression plot reveals higher explained variance (R^2) using multiple regressions incorporating pairs of features compared to simple regressions utilizing individual drought features as explanatory variables. For instance, for one potential predictor's response (i.e., the diagonal line of the upper regression plot), drought offset, taken as the predictor, explains 15 % ($R^2 = 0.15$) of the annual BA with a significant p-value of 0.02. Similarly, drought duration appears to be significantly correlated to BA (p-value = 0.04), although with a lower explained variance than drought offset ($R^2 = 0.11$). Both linear models, with positive bootstrapped slope coefficients, reveal that when drought duration increases or ends later in the season, the area burned is larger.

Our regression plot also demonstrates that incorporating pairs of drought features could improve the explanatory power compared to single explanatory variables. This is exemplified by the MLR model combining drying rate and drought offset of the same year (i.e.,

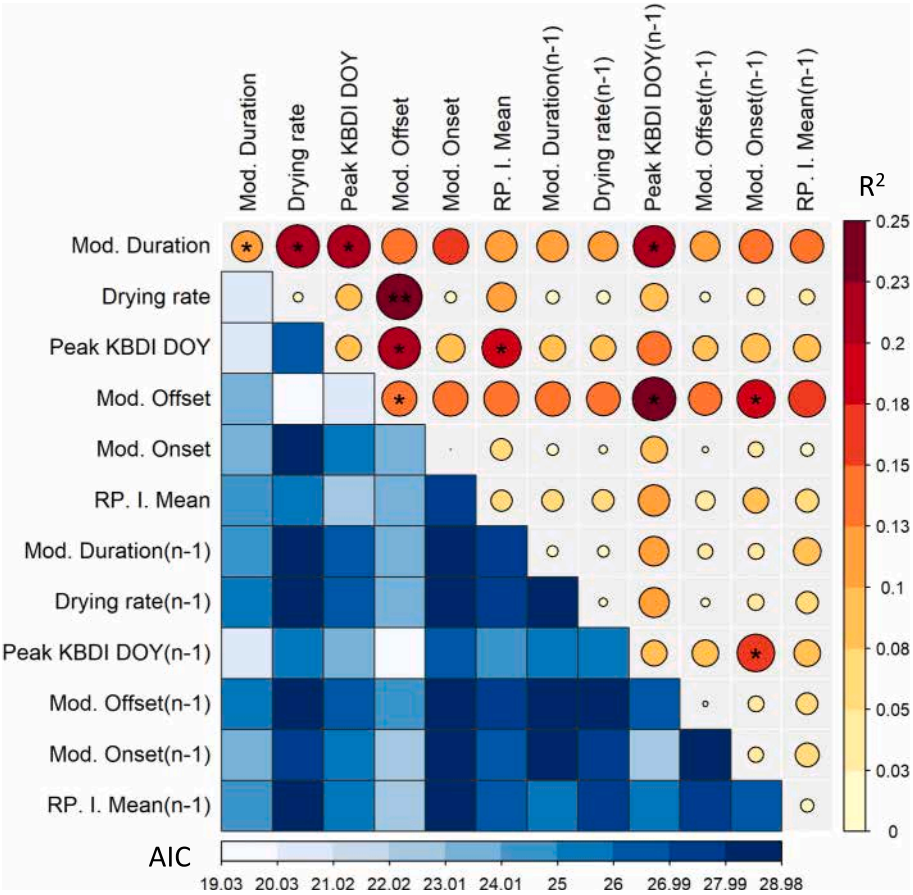

Fig. 5. Relationships between the six selected drought features and their lagged values by one year (*n-1*) with the detrended log10(BA). The color value and circle size in the upper diagonal cells are proportional to the range of the explained variance (R^2). Large circles colored with dark red are models with higher explained variance compared to others, which are colored with sequential shades from yellow to orange. Significant codes for *p*-values: 0.001 as '***', 0.01 as '**', 0.05 as '*', and non-significant as ''. The lower half of the diagonal provides the AIC numerical values for each developed model, using a sequential color scale from dark blue (highest AIC value) to very pale blue (lowest AIC value).

coincident drought year), which achieved the highest explained variance ($R^2 = 0.25$, p-value = 0.008). The 95 % confidence interval (CI) for the R^2, obtained via bootstrapping, ranges from 0.10 (lower CI bound) to 0.42 (higher CI bound). We conclude that both features synergistically act as positive explanators to the interannual variability of BAs. Other MLR models, with $R^2 \sim 0.20$ and featuring similar 95 % CI ranges for R^2, along with two statistically significant predictors, also appear in the regression plot and are summarized in Table 3.

Among others, drought duration combined either with the drying rate, the peak drought day of the coincident, or the peak drought day of the previous year, is statistically significant, with an explained variance of 0.23, 0.22, and 0.21 respectively. As secondary explanators, mean intensity of autumn rainfall pulses (RP·I mean, model 5) and earlier peak drought appear negatively correlated with BA, confirming the effectiveness of episodic rainfall pulses events at the end of the dry season in reducing burned area.

We'll note that a delayed peak drought day of the antecedent year (Peak KBDI DOY *n-1*, model 3 and 6) also leads to reduced BA in the year *n*. Taken together, the statistical analysis reported here points out that same-summer drought conditions exert a dominant influence on the areas burned by fires compared to the less influential association observed with antecedent drought conditions (*n-1*).

3.2. Wheat yield /drought relationship assessment

We investigated the relationship between drought features and wheat yield over the selected drought features matching the crop calendar.

Two statistically significant models (with p-values <0.05) capture the impact of coincident (year *n*) and antecedent (year *n-1*) drought features on wheat yields (Fig. 6). The first model includes the previous year autumn rainfall pulses (RP. I. Mean *n-1*) and the coincident year soil moisture drying rate occurring in spring during the growing period as the explanatory variables. The second model includes the previous year autumn rainfall with the current year drought onset as the explanatory variables. High daily drying rate (i.e., soil moisture depletion) and late-season drought onset during the growing season are negatively linked to wheat yield, hence causing harvest losses. However, in both models, the previous year autumn rainfall pulses intensity appears highly valuable for the sowing period, as increased rainfall pulses in year *n-1* lead to greater wheat yields in the next year (year *n)*. Both models exhibit an explained variance of 0.12 (p-value <0.05), with a 95 % CI ranging from 0.01 (lower CI bound) to 0.28 (higher CI bound).

Table 3
Performance of the best significant MLR models, developed between pairs of drought features and detrended log10 (BA). Rows report the predictors used in the developed model (Predictor 1 and Predictor 2), the slope coefficient of each predictor (Slope 1 and Slope 2), the model explained variance (Multiple R^2), and p-value significance levels.

Model	Predictor 1	Slope 1	Predictor 2	Slope 2	Multiple R^2	p-value
1	Mod. Duration	0.31	Drying rate	0.25	0.23	0.015
2	Mod. Duration	0.22	Peak KBDI DOY	0.13	0.22	0.017
3	Mod. Duration	0.22	Peak KBDI DOY (n-1)	- 0.13	0.21	0.02
4	Peak KBDI DOY	0.11	Mod. Offset	0.17	0.22	0.017
5	Peak KBDI DOY	0.15	RP. I. Mean	- 0.24	0.18	0.03
6	Mod. Offset	0.18	Peak KBDI DOY (n-1)	- 0.13	0.23	0.014

3.3. Tree ring / drought assessment along altitudinal gradient

We investigate here the tree-ring and drought relationship for the six sampling sites covering an altitudinal transect ranging from Wadi Balat (1170 m above sea level (asl)) to Bsharri (1940 m asl). Accordingly, six regression plots between pairs of drought features and tree-ring width chronologies are produced for each site (Figs. 7 a-f).

Wadi Balat (WB) and Herch Ehden (HE) sites (Fig. 7a, b), which are situated at the lowest altitudes compared to the other sites (Table 2), share approximately similar responses to drought features, more particularly regarding drought onset, which has the most statistically significant influence (HE p-value = 0.0002, and p-value = 0.0001 for WB) on the tree-ring growth of *Abies cilicica* and *Cedrus libani*, when considered alone as the single explanatory variable. The late-season drought onset reveals a positive association with tree-ring radial growth ($R^2 = 0.3$), while an early drought onset is negatively associated with tree-ring growth. In both sites, the 95 % CI for the bootstrapped explained variance ranges between 0.10 and 0.50. As a secondary explanatory factor, drought duration appears more statistically significant at the WB site (p-value = 0.004), exhibiting a higher explained variance ($R^2 = 0.19$) compared to the HE site ($R^2 = 0.10$), which shows less statistical significance (p-value = 0.04). Both sites highlight the negative association between longer drought duration (and accordingly drought severity) and decreased tree radial growth.

When both dimensions (duration and onset) are combined in a single model, the lowest site (WB) shows the highest statistically significant explained variance ($R^2 = 0.33$, p-value = 0.0004) compared to the HE site ($R^2 = 0.28$ and p-value = 0.001). At both sites, the explained variance is mostly dominated by drought onset, with a minor contribution of drought duration. We will note that other drought features do not have the same meaningful difference at the two sites (WB and HE). For instance, late-season rainfall pulses (RP. I. Mean) combined with drought onset of the same year are statistically significant in both sites, but only positively associated with tree-ring growth at the WB site. Interestingly, both sites have the same pattern of positive and statistically significant association (p-value = 0.0005) between the previous year's drought onset (Mod. onset *n-1*) and the current year's drought onset, which explains 32 % of tree-rings variability, where 95 % CI for bootstrapped R^2 ranges between 0.15 and 0.50.

When transitioning to a slightly higher altitude at the Maaser Al Shouf site (1700 m asl), drought duration becomes the most influential and statistically significant feature (p-value = 0.0006) negatively explaining 25 % ($R^2 = 0.25$) of tree-ring variability (95 % CI ranges between 0.10 and 0.46), while drought onset appears less statistically significant in affecting tree radial growth (p-value = 0.01, $R^2 = 0.14$). However, at this site, it is noteworthy to mention that drought duration also appears highly statistically significant (p-value <0.01) when combined with all the coincident and antecedent season drought features, with a statistical explained variance varying between 0.25 and 0.30 (Fig. 7c).

At the Barouk site (1775 m asl), with lower explained variance ($R^2 = 0.12$) and statistical significance (p-value = 0.03), drought duration is still the most influential feature on tree-ring growth when taken alone or even when combined with the previous year drought duration ($R^2 = 0.18$, p-value = 0.02) or onset ($R^2 = 0.20$, p-value = 0.01) (Fig. 7d).

At the Arz Jaj site (1780 m asl), one pair of drought features previous year drought onset (Mod. onset *n-1*) and mean rainfall pulses intensity (RP. I. mean *n-1*), positively and significantly explains 33 % ($R^2 = 0.33$) of tree-ring growth of the next year (Fig. 7e).

Finally, at the highest elevated site (Bsharri at 1940 m asl), drought duration and offset remain statistically significant (p-value = 0.01) when taken alone as predictors, but with a low explained variance (R2 = 0.12). However, when both are combined with the peak drought day of the previous season (Peak KBDI DOY *n-1*), the explained variance increases by 8 % ($R^2 = 0.20$) with approximately the same significance level (Fig. 7f).

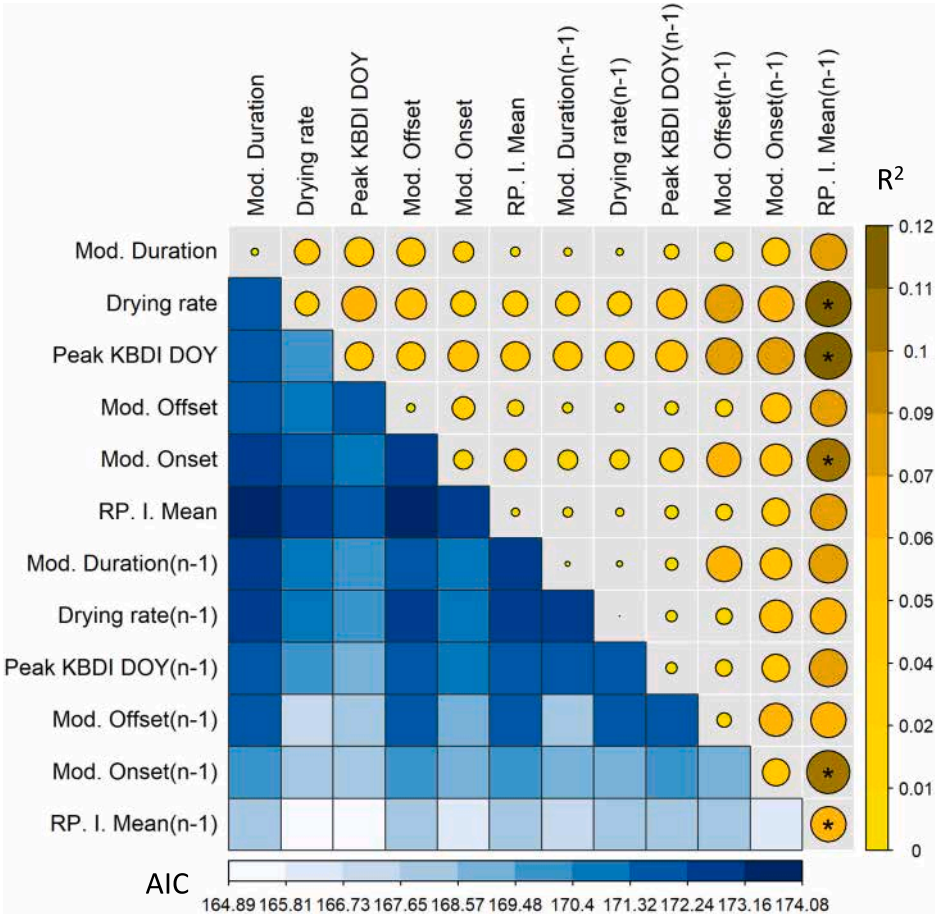

Fig. 6. Relationships between drought conditions prior (sowing period, year *n-1*) to the wheat growing season and drought conditions along the wheat growing season (year *n*) with the winter wheat yields. The color value and circle size in the upper diagonal cells (sequential colors from bright yellow to darker orange) are proportional to the range of the explained variance (R^2). Significant codes for *p*-values: 0.001 as '***', 0.01 as '**', 0.05 as '*', and non-significant as ''. The lower half of the diagonal provides the AIC numerical values for each developed model, using a sequential color scale from dark blue (highest AIC value) to very pale blue (lowest AIC value).

We conclude here on the progressive switch of drought feature contribution to tree radial growth from drought onset at lower altitudes to drought duration at higher altitudes.

3.4. Yearly drought features synchrony patterns across bio-climatic regions of Lebanon

We could previously show that agro-environmental variables are related to different combinations of drought facets. In turn, at the national level, we question here how to provide a synthetic yearly drought impact assessment index. Here, we analyzed how our key impactful drought features might be correlated and thus synchronized, so that some years could be qualified as hydrologically harmful for agro-environmental services when concomitant positive (or drier) drought features anomalies occur.

We can infer from Fig. 8 that drought features are hardly all concomitantly negative. This result suggests that, during climatically similar years, certain drought facets can have contrasting (positive or negative) asynchronous impacts on fire, plant growth or crop yield. We observed this pattern consistently across all bioclimatic zones of Lebanon. When summing up DF anomalies in an integrated drought feature severity index (DFSI) we could better capture particular years as 1998, 2007, 2008, 2010, and 2013 with the highest positive values, as a result of synchronous positive values in most drought feature (e.g., the synchronous harmful effect of drought duration, onset, offset, and rainfall pulses mean intensity concomitating in the year 2008). Additionally, we show an asynchronized pattern between the yearly calculated DFSI and precipitation anomalies across all bioclimatic zones, which indicates that relying solely on standardized precipitation indices may not fully capture the variability across the six functionally-targeted drought features considered in this study, nor the full spectrum of their associated agro-environmental threats. Drought features variability across bioclimatic zones aren't solely driven by precipitation amount, even if precipitation is the primary driver of soil drought, and depend more on an interplay of interactive factors, such as their temporal distribution and the daily temperature fluctuation. Yet, drought features are mostly not synchronized across the three studied bioclimatic zones covering the Lebanese territory, so that concomitant agro-environmental threats are relatively rare over our ecologically diverse region, as illustrated in Fig. 9.

4. Discussion

4.1. Agro-environmental functional meaning of yearly drought features

Our results reveal that the interannual variability of BA in Lebanon from 1984 to 2019 is predominantly and significantly correlated with both the rate of soil moisture depletion during drought onset and the timing of drought offset at the end of the dry season. It is noteworthy to mention that this MLR model explained variance ($R^2 = 0.25$) remains lower compared to other national and regional studies, which report values ranging from 0.40 to 0.80 of explained variability over the

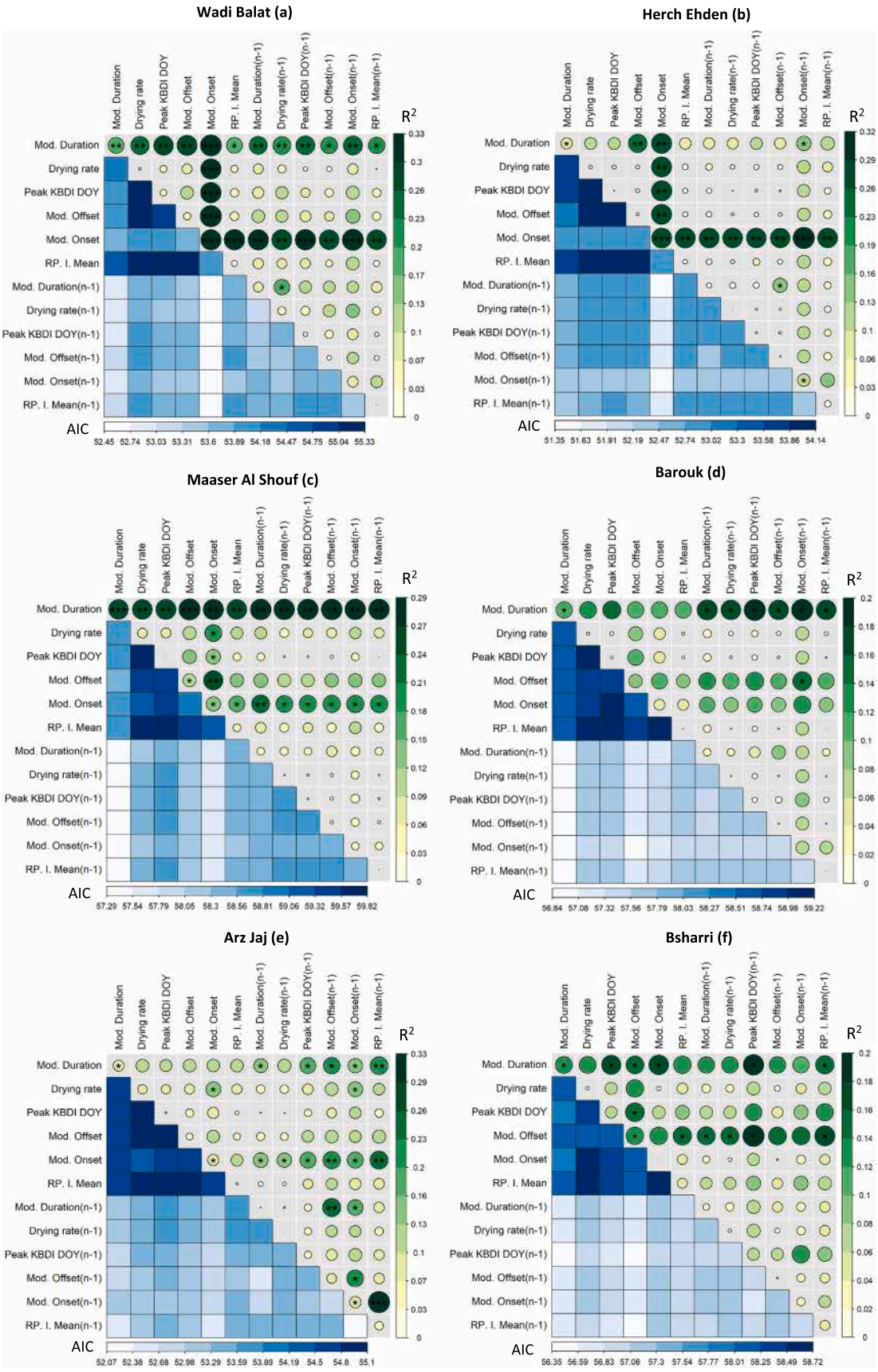

Fig. 7. Relationships between drought conditions prior and along the tree ring growing season with tree-ring width. The color value and circle size in the upper diagonal cells (sequential colors from light yellow to dark green) are proportional to the range of the explained variance (R^2). Significant codes for *p*-values: 0.001 as '***', 0.01 as '**', 0.05 as '*', and non-significant as ''. The lower half of the diagonal provides the AIC (here AIC/10 for space limitation) numerical values for each developed model, using a sequential color scale from dark blue (highest AIC value) to very pale blue (lowest AIC value).

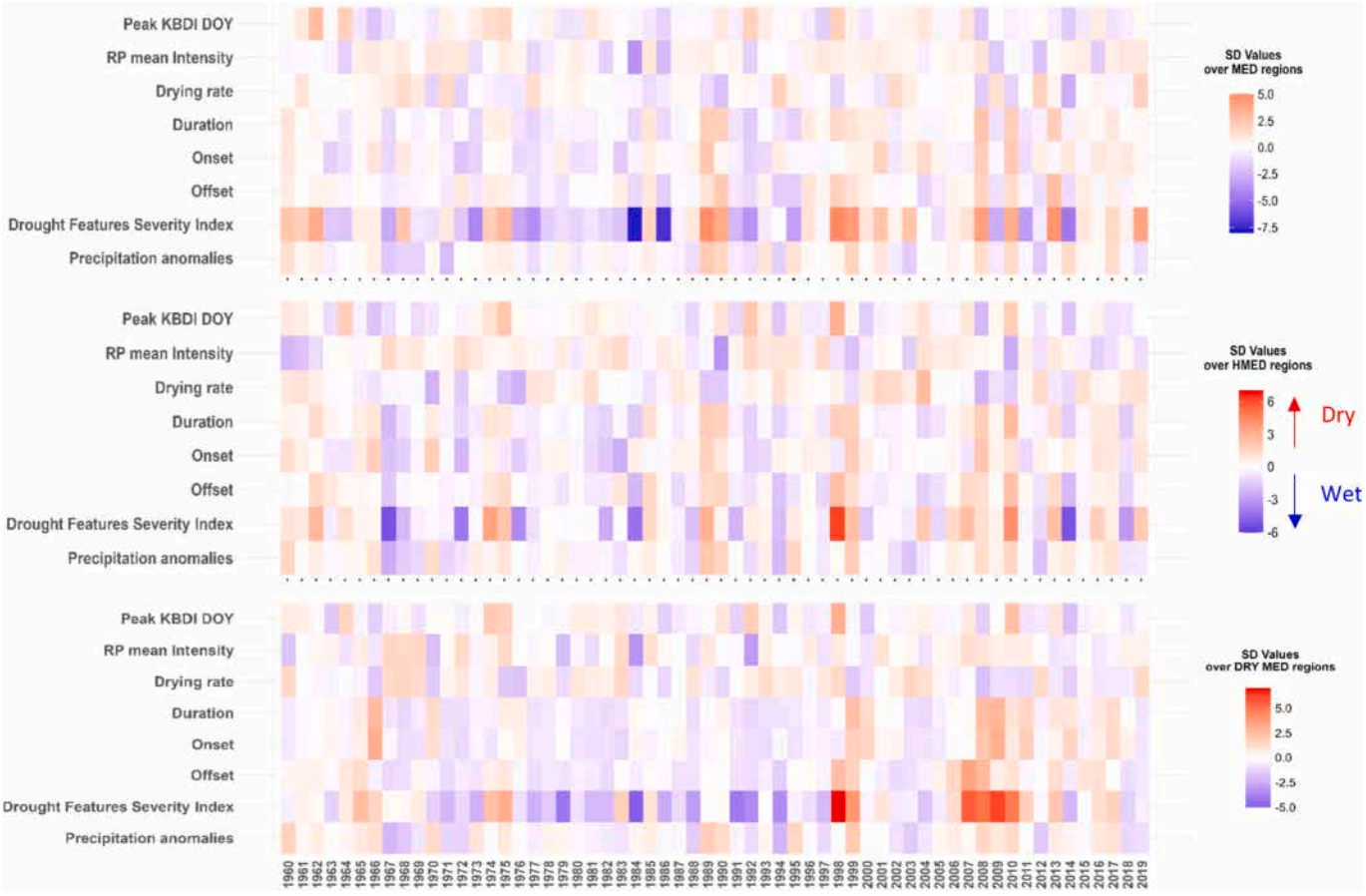

Fig. 8. Heat maps illustrating the time series of the standardized yearly extracted drought features (Drought Duration, Onset, Offset, Peak Drought Day, Drying Rate, and Rainfall Pulses Mean Intensity), their summation as a Drought Features Severity Index (DFSI), precipitation anomalies, and interannual synchronization patterns across the country's different drought-type regions: a) coastal MED (upper heat map), b) mountainous HMED (middle heat map), and c) arid DRY-MED (lower heat map). Harmful drought conditions are depicted in shades of red, while conditions with minimal or no impact are shown in shades of blue.

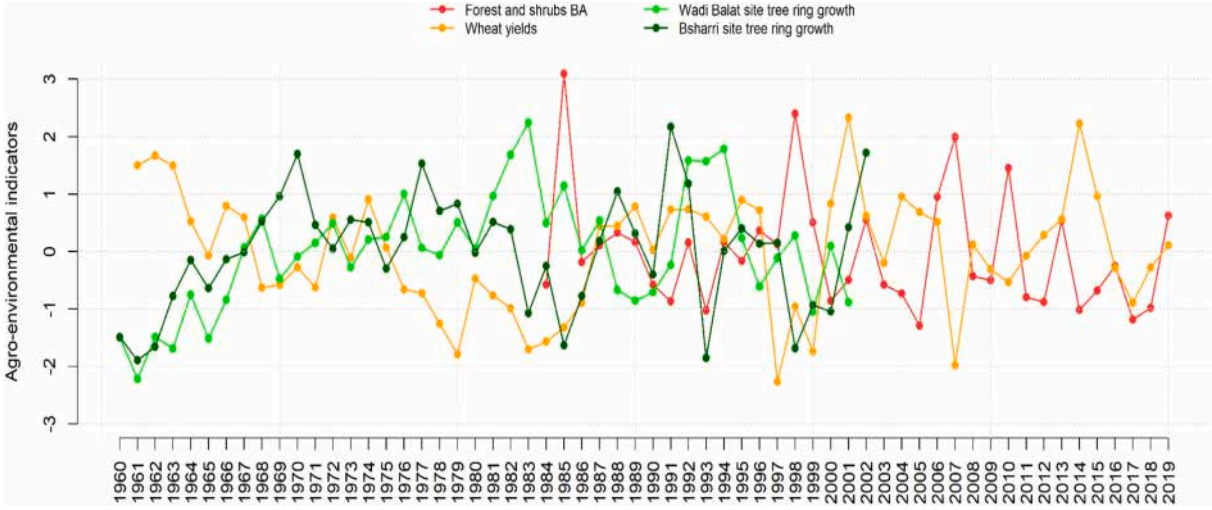

Fig. 9. Time series (in scaled values) over the 1960–2020 period of forests and shrubs burned areas (red), winter wheat annual yields (orange), and tree-ring chronology at two sites: Wadi Balat (lowest altitude, green) and Bsharri (highest altitude, dark green).

Mediterranean basin due to drought assessment using the SPEI index (Turco et al., 2017), although the most drought-prone southern Mediterranean countries experienced low to no-correlation in these analyses. In Lebanon, this lower explained variance may be due to the close relationship between BA variability and other anthropogenic factors, as noted by Majdalani (2023) and Mhawej et al. (2016, 2017). Additionally, the number of heat waves during the dry season might contribute more importantly than the considered drought features when drought is recurrent (Belhadj-Khedher et al., 2020; Ruffault et al., 2020). A faster drying rate of soil moisture during the drought development stage (i.e.,

spring and early summer seasons), in response to reduced or less intense spring precipitation and rising temperatures, could rapidly deplete soil moisture content, due to increasing atmospheric evaporative demand, leaving the herbaceous layer more flammable due to less water content in their leaves and tissues (Cardil et al., 2019; Jacobson et al., 2022; Turco et al., 2019; Westerling et al., 2006). Concomitantly, a delayed drought offset (i.e., during the months of October and November), contributes to prolonged and severe soil desiccation conditions. This extends the window of opportunity for more wildfires to occur during these two months (Majdalani et al., 2022; Richardson et al., 2022; Salloum and Mitri, 2014). Majdalani et al. (2022) specifically identified October and November as the peak fire months for the Lebanese Mediterranean forests and shrublands, a particular case within the Mediterranean basin, where summer months experience high air relative humidity while autumn experience drier air conditions. The delayed appearance of autumnal precipitations has also been evidenced in other Mediterranean areas (Cayan et al., 2022; Goss et al., 2020; Luković et al., 2021; Swain, 2021), extending fire-prone periods and leading to a larger cumulated burned area over the year. However, drought duration or severity might be more of a reliable index in other areas (Carvalho et al., 2021; Urbieta et al., 2015).

Regarding agricultural production, mostly located in the eastern part of the country in the Bekaa valley, we identified contrasted drought features occurring during the crop calendar and affecting the annual yield of winter wheat. Our analysis reveals that wheat yield of a particular year *n* is affected by drought conditions at the different stages of crop establishment. The key time periods are: October–December of the previous year (year *n-1)* when sowing starts and January–June of the current year (year *n)* during the growth and maturation. Our findings infer that an adequate soil moisture during the sowing period, captured by the significant contribution of rainfall pulses of year *n-1*, is essential for successful germination and seedling establishment (Bouras et al., 2020; Latiri et al., 2010; Pook et al., 2009; Wang et al., 2016), while a prolonged soil desiccation of year *n-1* due to delayed or insufficient autumn rainfall can hinder germination and root growth (Latiri et al., 2010; Peña-Gallardo et al., 2019; Yu et al., 2018). We also found that accelerated drying rates of soil moisture of year *n* coincide with insufficient spring rainfall, particularly during April and May (Páscoa et al., 2017; Tigkas and Tsakiris, 2015). This deficiency falls short of meeting the water demands of wheat crops during critical developmental stages when the photosynthetic activity peaks, surpassing earlier growth phases (Karam et al., 2009). In addition, our findings concur with previous ones showing that drought onset occurring during the end of the growing season (May and June), coinciding with the grain filling period, constraint wheat production in the Mediterranean region (Del Moral et al., 2003; Yang et al., 2020; Yu et al., 2018). Overall, our results indicate that features of drought from previous year (i.e., rainfall pulses *n-1*) and from current year (i.e., drought onset or drying rate *n*) can both contribute to predict wheat production at the national level. But it is worth noting that, although the developed models demonstrate statistically significant relationships between drought features and detrended winter wheat yield (p-value <0.05), the explained variance of these models is relatively low ($R^2 = 0.12$) compared to other regional and global studies. For instance, Peña-Gallardo et al. (2019) reported correlation values between different drought accumulation periods and wheat yields ranging between 0.41 and 0.6 at the district level in Spain using the SPEI index, and Leng and Hall (2019) reported an $R^2 = 0.25$ on a global scale when using the SPI drought index. Our results could be explained by the fact that, in Lebanon, >50 % of the wheat cultivated areas are irrigated, especially in the areas where rainfall fails to provide sufficient water thus, alleviating multifaceted drought impacts (Verner et al., 2018). Also, our results suggest, however, that irrigation may not be sufficient to totally alleviate drought impacts on yield. In the Bekaa valley, the primary wheat production area in Lebanon, irrigation is still conducted in a traditional way, rather than based on meteorological data or technological sensors (Abi Saab et al., 2019b). In addition, the variability in crop yield can also be attributed to other biotic and abiotic factors. For instance, spring frost, which we did not account for, was found to have detrimental impact on crop growth and productivity within the Bekaa valley (Abi Saab et al., 2019a).

We finally captured the sensitivity of tree radial growth to key drought facets. We could identify that, according to altitude (correlated to decreasing air temperatures and PET or increasing precipitation amount), tree growth responded to contrasted drought features, in line with the source (carbon assimilation) vs sink (non-photosynthetic) limitation hypothesis (Cabon et al., 2020; Guillemot et al., 2015; McDowell et al., 2008). In upper altitudes, drought duration was the main driver, while in lower altitudes, drought onset progressively appeared as the main driver. These results align with the findings recently reported by Cabon et al. (2024) across altitudinal gradients under Mediterranean climate, where limitations imposed by biophysical limitations (e.g., cambial cell division and development) at drier sites overpass the limitation imposed by carbon assimilation over the dry season in upper altitudes. In the highest site in altitude, Bsharri, the relationship between stem growth and drought duration can be attributed to the "carbon starvation" hypothesis, as a result of reduced photosynthesis when trees close their stomata and reduce carbon exchanges with the atmosphere, thus disrupting sugar transport within the phloem, limiting carbohydrate utilization and, consequently, promoting growth reduction (Cabon et al., 2024; Güney et al., 2017; McDowell et al., 2022). At the lower altitude sites, Wadi Balat and Herch Ehden, the correlation between stem growth and drought onset aligns more closely with the sink hypothesis. These findings are consistent with conclusions previously demonstrated by Güney et al. (2015, 2020), Lempereur et al. (2015), and Delpierre et al. (2016) revealing that the weather conditions prevailing during the period of most linear growth (spring months) are more crucial for defining the final ring widths and that drought onset is a keystone information for this agro-environmental sector. We also identified that at Wadi Balat, Herch Ehden, and Maaser Al Shouf sites, the drought conditions from the previous year seem to exert a significant influence on subsequent year's growth. Both drought onsets in the preceding year (Mod. onset *n-1*) and in the subsequent year can positively influence the formation of wider tree rings at the Wadi Balat and Herch Ehden sites. This result highlights the potential role of the preceding year (*n-1*) in shaping carbon balance and reserves. These reserves may be strategically utilized by trees in the subsequent year (*n*) to produce wider growth rings, particularly under delayed drought onset conditions (Cabon et al., 2024). The observed negative influence of the previous year's drought on subsequent growth aligns with the drought legacy effects, highlighting the enduring impacts of multifaceted drought occurrence on tree growths (Gao et al., 2018).

4.2. *Asynchrony of drought features as a driver of stability in agro-ecosystem functioning and threats*

One of our main result shows that drought features and their negative impacts on ecological and agronomic functions and processes are not correlated and, therefore, asynchronous at the local scale with non-concomitant extremes. This result leads to the key conclusion that a year considered as 'dry' based on annual or seasonal rainfall deficit (as usually performed Hendrawan et al., 2022, 2023), hides a more complex picture regarding its various facets and the asynchrony of their impacts on eco and agroecosystems. In our study area, we showed that drought features don't all reach high values at the same time (or year). Because different features affect different ecosystem functions and processes, we can expect that shocks/anomalies across different vegetation types don't happen synchronously, lowering the risk of triggering regional multi-crisis events (Homer-Dixon et al., 2015). Our multifaceted drought assessment framework then brings new insights for ecosystem synchrony analysis, an emerging property to elucidate ecosystem response to global change (Vagnon et al., 2024). Until now, species (crop or tree) diversity has been shown to drive agro- or ecosystem stability across

interannual climate variability (Grossiord et al., 2014; Renard et al., 2023; Renard and Tilman, 2019; Schnabel et al., 2021), through complementarity mechanisms inferred from the interspecific variability in water stress response (Liu et al., 2024). More specifically, Valencia et al. (2020) suggested that the synchrony in species responses to climate overrides species richness in stabilizing plant community functioning. While research has explored the role of the multiple facets of biodiversity (richness, evenness) on the ecosystem's stability (Craven et al., 2018), as a future avenue of research, we suggest here that the asynchrony in the multiple facets of droughts should be further assessed as a climate driver of ecosystem's stability and as a potential driver of species leaf and root traits (Skelton et al., 2015; Sun et al., 2024). Providing drought facets tailored to agronomists and ecologists, corresponding to acknowledged critical thresholds for plant functioning, should facilitate broader adoption compared to sometimes obscure drought indices (Slette et al., 2019). Moreover, the tool is generic enough to be used on any soil water content generated from empirical or process-based models using climate time series, or remotely sensed plant or soil moisture content over bioclimates experiencing a single drought period as the Mediterranean (Elias et al., 2024). We tested these effects on wheat yield, forest fires, and tree growth, but any other agro-environmental issue as Mediterranean rainfed agriculture (olive, grape wine, barley, and pine seeds) (Trabelsi et al., 2022), pasture and grazing (Iglesias et al., 2016), irrigation demand (Xing et al., 2020), or forest management such as tree mortality (Allen et al., 2015), could be assessed with this framework.

4.3. From local to regional drought synchrony through atmospheric oscillations

Our study combined three agro-environmental threats over the national territory of Lebanon, showing differential responses to drought facets, but also encompassing different regions with contrasted climates. Forest fires mostly happen in the coastal region (Majdalani et al., 2022), while major forests cover the mountainous areas and wheat crops are mostly located in the northeastern part of the country (CNRS-L., 2019). We highlighted the role of contrasted and asynchronous drought facets in driving agro-environmental threats during extreme events, enhanced when they happen concomitantly, but our study accounts for the spatial asynchronies in climate variability and the subsequent occurrence of drought facets. At the global scale, synchronized crop failure is a major threat to food security when extreme climatic events occur concomitantly over major global cropping areas (Mehrabi and Ramankutty, 2019) in the context of global market. At the national level as in Lebanon, this spatial synchrony of drought events might affect national food security, particularly in countries under economic crisis as currently happening (Abou Ltaif et al., 2024; Ali, 2024). Detecting synchrony in pixel-level drought facets, or area-weighted anomalies as in severity-area-duration approaches (Andreadis et al., 2005; Zhou et al., 2020) should bring fruitful information on food or environmental security related to drought events.

This spatial synchrony can reveal synoptic large-scale events. For example, tree growth synchrony (or drought onset and drought duration as revealed in our analysis) has been shown to be an effective indicator of large-scale climate extremes (Jia et al., 2024), mostly related to atmospheric oscillations potentially affecting concomitantly all ecosystems (Krawczyk et al., 2020). This regional synchrony, extending the concept of drought to its spatial extent, is a major indicator of historical climate change and megadrought occurrence with high regional socio-ecological impacts (Ionita et al., 2021; Sharma and Mujumdar, 2017) that should be further investigated through drought features in the context of climate change and agro-environmental impact assessment.

4.4. Toward a compound drought facets index

Finally, our analysis could reveal the differential impacts of various drought facets on key agro-environmental threats over Lebanon and their regional temporal and spatial variability across the country. Increasing need for early warning of climate threats (Hermans et al., 2022) or long-term country strategies for sustainable development goals under climate change scenarios have been raised (Xue et al., 2024). While single drought indices appear insufficient, multiple indices could bring confusion. Synthetic compound indices have been proposed for drought, mostly combining drought types (Tramblay et al., 2020): meteorological, hydrological, and agricultural droughts (Ali et al., 2022; von Matt et al., 2024; Wu et al., 2022). For the Middle East and North Africa more specifically, Bergaoui et al. (2024) developed a Composite Drought Index (CDI) combining remote sensing and modeled data inputs, reflecting anomalies in precipitation (through SPI calculation), vegetation (NDVI index), soil moisture (root-zone soil moisture anomaly), and evapotranspiration. These compound indices were even complexified by combining drought with heat indices as a major critical information for agro environmental disruptions (Hao et al., 2020; Hosseinzadehtalaei et al., 2024; Li et al., 2021). Elias et al. (2024) highlighted the significance of this approach in DFEAT development perspectives. Yet, building on this approach, we propose here a compound index of drought facets. By revealing the functional role of each facet on agro- and ecosystems, we suggest that a compound drought facet index could bring synthetic information on potential concomitant threats leading to crises. Therefore, we could provide an efficient drought assessment tool and framework so that policymakers and land managers will be better equipped to more effectively diagnose the climatic drivers of agro-environmental issues within the key affected sectors. Furthermore, providing climate change projections of frequency and intensity of drought features can significantly enhance preparedness and raise awareness of the potential effects of future classified ‘harmful’ hydrological years on the country's primary agro-environmental sectors. This approach fosters a more sustainable and adaptive future management framework to mitigate national agro-environmental crises in the country, particularly in the context of socio-political instability (Ali, 2024; Kharroubi et al., 2021).

5. Conclusion

This study proposed a comprehensive characterization of yearly multifaceted drought events, leveraging daily simulated soil water balance. We could also provide valuable insights on drought features' functional meaning for major agro-environmental threats in the typical Mediterranean agro-ecosystems over Lebanon. By constructing parsimonious Multiple Linear Regression (MLR) models that incorporate pairs of drought features from both the current and preceding year, we were able to assess their statistically significant effects on each target variable. Our findings substantiate our initial hypothesis that the interannual variability in agro-environmental threats is multifactorial and that combined drought features provide a superior explained variance compared to individual features. Additionally, our results validate our second hypothesis regarding the differential weighting of various drought features in relation to the target variables. By leveraging these correlations, we concluded on the significant role of drought facets asynchrony in buffering climate impacts leading to multiple and concomitant agro-environmental crisis. Synchronous disturbances actually constitute a major under-investigated threat with potentially aggravating cascading effects (Burton et al., 2020), more hardly handled under socio-political and economic instability as currently in Lebanon and other Mediterranean countries (Diourane and Talbi, 2024), a major concern for disaster reduction goals of the Sendai Framework (Peters, 2024; UNDRR, 2015).

CRediT authorship contribution statement

Georgie Elias: Writing – original draft, Visualization, Software, Methodology, Investigation, Formal analysis, Data curation,

Conceptualization. **Georgia Majdalani:** Writing – review & editing, Visualization, Software, Methodology, Formal analysis. **Delphine Renard:** Writing – review & editing, Conceptualization. **Ghaleb Faour:** Writing – review & editing, Supervision, Resources, Funding acquisition, Conceptualization. **Florent Mouillot:** Writing – review & editing, Validation, Supervision, Resources, Project administration, Methodology, Funding acquisition, Conceptualization.

Declaration of competing interest

The authors declare that they have no known competing financial interests or personal relationships that could have appeared to influence the work reported in this paper.

Acknowledgments

The authors acknowledge the National Council for Scientific Research of Lebanon (CNRS-L), the French Embassy in Lebanon and Campus France for granting a doctoral fellowship to Georgie Elias (SAFAR program). The authors also express their gratitude to Dr. Ramzi Touchan for his constructive review of our work and for his valuable assistance in understanding the time series of tree rings. The authors would also like to thank the three anonymous reviewers for their thorough revisions, insightful remark, and constructive comments, which have significantly contributed to improving the quality of this manuscript.

Data availability

Data will be made available on request.

References

Abi Saab, M.T., Houssemeddine Sellami, M., Giorio, P., Basile, A., Bonfante, A., Rouphael, Y., Fahed, S., Jomaa, I., Stephan, C., Kabalan, R., 2019a. Assessing the potential of cereal production systems to adapt to contrasting weather conditions in the Mediterranean region. Agronomy 9 (7), 393. https://doi.org/10.3390/agronomy9070393.

Abi Saab, M.T., Jomaa, I., Skaf, S., Fahed, S., Todorovic, M., 2019b. Assessment of a smartphone application for real-time irrigation scheduling in Mediterranean environments. Water 11 (2), 252. https://doi.org/10.3390/w11020252.

Abou Ltaif, S.F., Mihai-Yiannaki, S., Thrassou, A., 2024. Lebanon's economic development risk: global factors and local realities of the shadow economy amid financial crisis. Risks 12 (8). https://doi.org/10.3390/risks12080122.

Akaike, H., 1974. A new look at the statistical model identification. IEEE Trans. Autom. Control 19 (6), 716–723. https://doi.org/10.1109/TAC.1974.1100705.

Alfaro-Sánchez, R., Camarero, J. J., Sánchez-Salguero, R., Trouet, V., & Heras, J. de L. (2018). How do droughts and wildfires alter seasonal radial growth in Mediterranean Aleppo pine forests? Tree-Ring Research, 74(1), 1–14. doi:https://doi.org/10.3959/1536-1098-74.1.1.

Ali, A., 2024. Displacement in place and the financial crisis in Lebanon. J. Refug. Stud. 37 (1), 201–219. https://doi.org/10.1093/jrs/fead076.

Ali, M., Ghaith, M., Wagdy, A., Helmi, A.M., 2022. Development of a new multivariate composite drought index for the Blue Nile River basin. Water 14 (6), 886. https://doi.org/10.3390/w14060886.

Allen, C.D., Breshears, D.D., McDowell, N.G., 2015. On underestimation of global vulnerability to tree mortality and forest die-off from hotter drought in the Anthropocene. Ecosphere 6 (8), 1–55. https://doi.org/10.1890/ES15-00203.1.

Allen, C.D., Macalady, A.K., Chenchouni, H., Bachelet, D., McDowell, N., Vennetier, M., Kitzberger, T., Rigling, A., Breshears, D.D., Hogg, E.T., 2010. A global overview of drought and heat-induced tree mortality reveals emerging climate change risks for forests. For. Ecol. Manag. 259 (4), 660–684. https://doi.org/10.1016/j.foreco.2009.09.001.

Andrade, C., Bugalho, L., 2023. Multi-indices diagnosis of the conditions that led to the two 2017 major wildfires in Portugal. Fire 6 (2), 56. https://doi.org/10.3390/fire6020056.

Andreadis, K.M., Clark, E.A., Wood, A.W., Hamlet, A.F., Lettenmaier, D.P., 2005. Twentieth-century drought in the conterminous United States. J. Hydrometeorol. 6 (6), 985–1001. https://doi.org/10.1175/JHM450.1.

Aussenac, G., 2002. Ecology and ecophysiology of circum-Mediterranean firs in the context of climate change. Ann. For. Sci. 59 (8), 823–832. https://doi.org/10.1051/forest:2002080.

Awad, L., Fady, B., Khater, C., Roig, A., Cheddadi, R., 2014. Genetic structure and diversity of the endangered fir tree of Lebanon (Abies cilicica Carr.): implications for conservation. PLoS One 9 (2), e90086. https://doi.org/10.1371/journal.pone.0090086.

Barbero, R., Curt, T., Ganteaume, A., Maillé, E., Jappiot, M., Bellet, A., 2019. Simulating the effects of weather and climate on large wildfires in France. Nat. Hazards Earth Syst. Sci. 19 (2), 441–454. https://doi.org/10.5194/nhess-19-441-2019.

Belhadj-Khedher, C., El-Melki, T., Mouillot, F., 2020. Saharan hot and dry sirocco winds drive extreme fire events in Mediterranean Tunisia (North Africa). Atmosphere 11 (6), 590. https://doi.org/10.3390/atmos11060590.

Bergaoui, K., Fraj, M.B., Fragaszy, S., Ghanim, A., Hamadin, O., Al-Karablieh, E., Al-Bakri, J., Fakih, M., Fayad, A., Comair, F., 2024. Development of a composite drought indicator for operational drought monitoring in the MENA region. Sci. Rep. 14 (1), 5414. https://doi.org/10.1038/s41598-024-55626-0.

Beridze, B., Walas, Ł., Iszkuło, G., Jasińska, A.K., Kosiński, P., Sękiewicz, K., Tomaszewski, D., Dering, M., 2021. Demographic history and range modelling of the East Mediterranean Abies cilicica. Plant and Fungal Systematics 66 (2), 122–132. https://doi.org/10.35535/pfsyst-2021-0011.

Bhuyan, U., Zang, C., Menzel, A., 2017. Different responses of multispecies tree ring growth to various drought indices across Europe. Dendrochronologia 44, 1–8. https://doi.org/10.1016/j.dendro.2017.02.002.

Blauhut, V., Stahl, K., Stagge, J.H., Tallaksen, L.M., De Stefano, L., Vogt, J., 2016. Estimating drought risk across Europe from reported drought impacts, drought indices, and vulnerability factors. Hydrol. Earth Syst. Sci. 20 (7), 2779–2800. https://doi.org/10.5194/hess-20-2779-2016.

Bouras, E.H., Jarlan, L., Er-Raki, S., Albergel, C., Richard, B., Balaghi, R., Khabba, S., 2020. Linkages between rainfed cereal production and agricultural drought through remote sensing indices and a land data assimilation system: A case study in Morocco. Remote Sens. 12 (24), 4018. https://doi.org/10.3390/rs12244018.

Bouras, E.H., Jarlan, L., Er-Raki, S., Balaghi, R., Amazirh, A., Richard, B., Khabba, S., 2021. Cereal yield forecasting with satellite drought-based indices, weather data and regional climate indices using machine learning in Morocco. Remote Sens. 13 (16), 3101. https://doi.org/10.3390/rs13163101.

Burton, P.J., Jentsch, A., Walker, L.R., 2020. The ecology of disturbance interactions. BioScience 70 (10), 854–870. https://doi.org/10.1093/biosci/biaa088.

Cabon, A., Ameztegui, A., Anderegg, W.R., Martínez-Vilalta, J., De Cáceres, M., 2024. Probing the interplay of biophysical constraints and photosynthesis to model tree growth. Agric. For. Meteorol. 345, 109852. https://doi.org/10.1016/j.agrformet.2023.109852.

Cabon, A., Peters, R.L., Fonti, P., Martínez-Vilalta, J., De Cáceres, M., 2020. Temperature and water potential co-limit stem cambial activity along a steep elevational gradient. New Phytol. 226 (5), 1325–1340. https://doi.org/10.1111/nph.16456.

Canty, A., & Ripley, B. (2017). Package 'boot.' Bootstrap Functions. CRAN R Proj. https://www.vps.fmvz.usp.br/CRAN/web/packages/boot/boot.pdf.

Cardil, A., Vega-García, C., Ascoli, D., Molina-Terrén, D.M., Silva, C.A., Rodrigues, M., 2019. How does drought impact burned area in Mediterranean vegetation communities? Sci. Total Environ. 693, 133603. https://doi.org/10.1016/j.scitotenv.2019.133603.

Carvalho, N.S., Anderson, L.O., Nunes, C.A., Pessôa, A.C., Junior, C.H.S., Reis, J.B., Shimabukuro, Y.E., Berenguer, E., Barlow, J., Aragao, L.E., 2021. Spatio-temporal variation in dry season determines the Amazonian fire calendar. Environ. Res. Lett. 16 (12), 125009. https://doi.org/10.1088/1748-9326/ac3aa3.

Cayan, D.R., DeHaan, L.L., Gershunov, A., Guzman-Morales, J., Keeley, J.E., Mumford, J., Syphard, A.D., 2022. Autumn precipitation: the competition with Santa Ana winds in determining fire outcomes in southern California. Int. J. Wildland Fire 31 (11), 1056–1067. https://doi.org/10.1071/WF22065.

Choat, B., Brodribb, T.J., Brodersen, C.R., Duursma, R.A., López, R., Medlyn, B.E., 2018. Triggers of tree mortality under drought. Nature 558 (7711), 531–539. https://doi.org/10.1038/s41586-018-0240-x.

CNRS-L., 2019. *2017 Land Cover/Land Use Map of Lebanon Scale 1/20 000* [Map]. National Center of Scientific Research/National Center of Remote Sensing.

Core Team, R, 2021. R: A Language and Environment for Statistical Computing [Computer Software]. R Foundation for Statistical Computing, Vienna, Austria.

Coscarelli, R., Aguilar, E., Petrucci, O., Vicente-Serrano, S.M., Zimbo, F., 2021. The potential role of climate indices to explain floods, mass-movement events and wildfires in southern Italy. Climate 9 (11), 156. https://doi.org/10.3390/cli9110156.

Crausbay, S.D., Ramirez, A.R., Carter, S.L., Cross, M.S., Hall, K.R., Bathke, D.J., Betancourt, J.L., Colt, S., Cravens, A.E., Dalton, M.S., 2017. Defining ecological drought for the twenty-first century. Bull. Am. Meteorol. Soc. 98 (12), 2543–2550. https://doi.org/10.1175/BAMS-D-16-0292.1.

Craven, D., Eisenhauer, N., Pearse, W.D., Hautier, Y., Isbell, F., Roscher, C., Bahn, M., Beierkuhnlein, C., Bönisch, G., Buchmann, N., 2018. Multiple facets of biodiversity drive the diversity–stability relationship. Nature Ecology & Evolution 2 (10), 1579–1587. https://doi.org/10.1038/s41559-018-0647-7.

Davison, A. C., & Hinkley, D. V. (1997). Bootstrap methods and their application. Cambridge university press. https://books.google.com/books?hl=fr&lr=&id=4aCDbm_t8jUC&oi=fnd&pg=PR7&dq=Davison,+A.+C.+%26+Hinkley,+D.+V.+(1997)+Bootstrap+Methods+and+Their+Applications.+Cambridge+University+++Press,+Cambridge.+ISBN+0-521-57391-2&ots=m_3kbZ-16&sig=nBqkJywIUfm1edwzy-69mnXYHPc.

Del Moral, L.F.G., Rharrabti, Y., Villegas, D., Royo, C., 2003. Evaluation of grain yield and its components in durum wheat under Mediterranean conditions: an Ontogenic approach. Agron. J. 95 (2), 266–274. https://doi.org/10.2134/agronj2003.2660.

Delpierre, N., Berveiller, D., Granda, E., Dufrêne, E., 2016. Wood phenology, not carbon input, controls the interannual variability of wood growth in a temperate oak forest. New Phytol. 210 (2), 459–470. https://doi.org/10.1111/nph.13771.

Dickey, D.A., Fuller, W.A., 1979. Distribution of the estimators for autoregressive time series with a unit root. J. Am. Stat. Assoc. 74 (366a), 427–431. https://doi.org/10.1080/01621459.1979.10482531.

Dimitrakopoulos, A.P., Bemmerzouk, A.M., 2003. Predicting live herbaceous moisture content from a seasonal drought index. Int. J. Biometeorol. 47 (2), 73–79. https://doi.org/10.1007/s00484-002-0151-1.
Diourane, H., Talbi, L.F.-Z.A., 2024. Gestion des Crises dans les Pays en Développement: Une Analyse Comparative des Meilleures Pratiques Internationales. International Journal of Accounting, Finance, Auditing, Management and Economics 5 (12), 474–488. https://doi.org/10.5281/zenodo.14286198.
Dixon, G., Bullock, O., Adams, D., 2019. Unintended effects of emphasizing the role of climate change in recent natural disasters. Environ. Commun. 13 (2), 135–143. https://doi.org/10.1080/17524032.2018.1546202.
Elias, G., Faour, G., Mouillot, F., 2024. DFEAT: A multifaceted yearly drought FEature assessment tool from daily soil water content. J. Hydrol. 131700. https://doi.org/10.1016/j.jhydrol.2024.131700.
Fu, Z., Ciais, P., Wigneron, J.-P., Gentine, P., Feldman, A.F., Makowski, D., Viovy, N., Kemanian, A.R., Goll, D.S., Stoy, P.C., 2024. Global critical soil moisture thresholds of plant water stress. Nat. Commun. 15 (1), 4826. https://doi.org/10.1038/s41467-024-49244-7.
Ganatsas, P., Antonis, M., Marianthi, T., 2011. Development of an adapted empirical drought index to the Mediterranean conditions for use in forestry. Agric. For. Meteorol. 151 (2), 241–250. https://doi.org/10.1016/j.agrformet.2010.10.011.
Gao, S., Liu, R., Zhou, T., Fang, W., Yi, C., Lu, R., Zhao, X., Luo, H., 2018. Dynamic responses of tree-ring growth to multiple dimensions of drought. Glob. Chang. Biol. 24 (11), 5380–5390. https://doi.org/10.1111/gcb.14367.
Gazol, A., Ribas, M., Gutiérrez, E., Camarero, J.J., 2017. Aleppo pine forests from across Spain show drought-induced growth decline and partial recovery. Agric. For. Meteorol. 232, 186–194. https://doi.org/10.1016/j.agrformet.2016.08.014.
Goss, M., Swain, D.L., Abatzoglou, J.T., Sarhadi, A., Kolden, C.A., Williams, A.P., Diffenbaugh, N.S., 2020. Climate change is increasing the likelihood of extreme autumn wildfire conditions across California. Environ. Res. Lett. 15 (9), 094016. https://doi.org/10.1088/1748-9326/ab83a7.
Granier, A., Bréda, N., Biron, P., & Villette, S. (1999). A lumped water balance model to evaluate duration and intensity of drought constraints in forest stands. Ecol. Model., 116(2–3), 269–283. doi:https://doi.org/10.1016/S0304-3800(98)00205-1.
Grossiord, C., Granier, A., Ratcliffe, S., Bouriaud, O., Bruelheide, H., Chećko, E., Forrester, D.I., Dawud, S.M., Finér, L., Pollastrini, M., Scherer-Lorenzen, M., Valladares, F., Bonal, D., Gessler, A., 2014. Tree diversity does not always improve resistance of forest ecosystems to drought. Proc. Natl. Acad. Sci. 111 (41), 14812–14815. https://doi.org/10.1073/pnas.1411970111.
Guillemot, J., Martin-StPaul, N.K., Dufrêne, E., François, C., Soudani, K., Ourcival, J.-M., Delpierre, N., 2015. The dynamic of the annual carbon allocation to wood in European tree species is consistent with a combined source–sink limitation of growth: implications for modelling. Biogeosciences 12 (9), 2773–2790. https://doi.org/10.5194/bg-12-2773-2015.
Güney, A., Kerr, D., Sökücü, A., Zimmermann, R., Küppers, M., 2015. Cambial activity and xylogenesis in stems of Cedrus libani A. Rich at different altitudes. *Botanical Studies* 56 (1), 20. https://doi.org/10.1186/s40529-015-0100-z.
Güney, A., Küppers, M., Rathgeber, C., Şahin, M., Zimmermann, R., 2017. Intra-annual stem growth dynamics of Lebanon cedar along climatic gradients. Trees 31 (2), 587–606. https://doi.org/10.1007/s00468-016-1492-4.
Güney, A., Zweifel, R., Türkan, S., Zimmermann, R., Wachendorf, M., Güney, C.O., 2020. Drought responses and their effects on radial stem growth of two co-occurring conifer species in the Mediterranean mountain range. Ann. For. Sci. 77 (4), 105. https://doi.org/10.1007/s13595-020-01007-2.
Haddad, E.A., Farajalla, N., Camargo, M., Lopes, R.L., Vieira, F.V., 2014. Climate change in Lebanon: higher-order regional impacts from agriculture. Region 1 (1), 9–24.
Haile, G.G., Tang, Q., Li, W., Liu, X., Zhang, X., 2020. Drought: Progress in broadening its understanding. WIREs Water 7 (2), e1407. https://doi.org/10.1002/wat2.1407.
Hajar, L., François, L., Khater, C., Jomaa, I., Déqué, M., Cheddadi, R., 2010. Cedrus libani (A. Rich) distribution in Lebanon: past, present and future. C. R. Biol. 333 (8), 622–630. https://doi.org/10.1016/j.crvi.2010.05.003.
Hao, Z., Hao, F., Singh, V.P., Ouyang, W., Zhang, X., Zhang, S., 2020. A joint extreme index for compound droughts and hot extremes. Theor. Appl. Climatol. 142 (1–2), 321–328. https://doi.org/10.1007/s00704-020-03317-x.
Hendrawan, V.S.A., Kim, W., Touge, Y., Ke, S., Komori, D., 2022. A global-scale relationship between crop yield anomaly and multiscalar drought index based on multiple precipitation data. Environ. Res. Lett. 17 (1), 014037. https://doi.org/10.1088/1748-9326/ac45b4.
Hendrawan, V.S.A., Komori, D., Kim, W., 2023. Possible factors determining global-scale patterns of crop yield sensitivity to drought. PLoS One 18 (2), e0281287. https://doi.org/10.1371/journal.pone.0281287.
Hermans, T.D.G., Šakić Trogrlić, R., Van Den Homberg, M.J.C., Bailon, H., Sarku, R., Mosurska, A., 2022. Exploring the integration of local and scientific knowledge in early warning systems for disaster risk reduction: A review. Nat. Hazards 114 (2), 1125–1152. https://doi.org/10.1007/s11069-022-05468-8.
Homer-Dixon, T., Walker, B., Biggs, R., Crépin, A.-S., Folke, C., Lambin, E.F., Peterson, G. D., Rockström, J., Scheffer, M., Steffen, W., 2015. Synchronous failure: the emerging causal architecture of global crisis. Ecol. Soc. 20 (3). https://doi.org/10.5751/ES-07681-200306.
Hoover, D.L., Bestelmeyer, B., Grimm, N.B., Huxman, T.E., Reed, S.C., Sala, O., Seastedt, T.R., Wilmer, H., Ferrenberg, S., 2020. Traversing the wasteland: A framework for assessing ecological threats to drylands. BioScience 70 (1), 35–47. https://doi.org/10.1093/biosci/biz126.
Hosseinzadehtalaei, P., Termonia, P., Tabari, H., 2024. Projected changes in compound hot-dry events depend on the dry indicator considered. Communications Earth & Environment 5 (1), 220. https://doi.org/10.1038/s43247-024-01352-4.
Hyndman, R. J., Athanasopoulos, G., Bergmeir, C., Caceres, G., Chhay, L., O'Hara-Wild, M., Petropoulos, F., Razbash, S., & Wang, E. (2020). Package 'forecast.' Online] Https://Cran. r-Project. Org/Web/Packages/Forecast/Forecast. Pdf http://cran.rediris.es/web/packages/forecast/forecast.pdf.
Iglesias, E., Báez, K., Diaz-Ambrona, C.H., 2016. Assessing drought risk in Mediterranean Dehesa grazing lands. Agric. Syst. 149, 65–74. https://doi.org/10.1016/j.agsy.2016.07.017.
Ionita, M., Dima, M., Nagavciuc, V., Scholz, P., Lohmann, G., 2021. Past megadroughts in Central Europe were longer, more severe and less warm than modern droughts. Communications Earth & Environment 2 (1), 61. https://doi.org/10.1038/s43247-021-00130-w.
Jacobson, T.W., Seager, R., Williams, A.P., Henderson, N., 2022. Climate dynamics preceding summer forest fires in California and the extreme case of 2018. J. Appl. Meteorol. Climatol. 61 (8), 989–1002. https://doi.org/10.1175/JAMC-D-21-0198.1.
Jia, H., Zheng, J., Yang, J., Lyu, L., Dong, Y., Fang, O., 2024. Tree-growth synchrony index, an effective indicator of historical climatic extremes. Ecol. Process. 13 (1), 55. https://doi.org/10.1186/s13717-024-00536-2.
Jomaa, I., Abi Saab, M.T., Skaf, S., El Haj, N., Massaad, R., 2019. Variability in spatial distribution of precipitation overall rugged topography of Lebanon, using TRMM images. Atmospheric and Climate Sciences 9 (3), 369–380. https://doi.org/10.4236/acs.2019.93026.
Karam, F., Kabalan, R., Breidi, J., Rouphael, Y., Oweis, T., 2009. Yield and water-production functions of two durum wheat cultivars grown under different irrigation and nitrogen regimes. Agric. Water Manag. 96 (4), 603–615. https://doi.org/10.1016/j.agwat.2008.09.018.
Keetch, J.J., Byram, G.M., 1968. *A drought index for forest fire control* (Vol. 38). US Department of Agriculture, Forest Service, southeastern Forest experiment …. https://books.google.com/books?hl=fr&lr=&id=zUiUwKYMq_8C&oi=fnd&pg=PA11&dq=keetch+byram+1968&ots=2omN2-rDRb&sig=jRdYqopcoLsHzlOl63zNyg-VFvc.
Kharroubi, S., Naja, F., Diab-El-Harake, M., Jomaa, L., 2021. Food insecurity pre-and post the COVID-19 pandemic and economic crisis in Lebanon: prevalence and projections. Nutrients 13 (9), 2976. https://doi.org/10.3390/nu13092976.
Klein, T., 2014. The variability of stomatal sensitivity to leaf water potential across tree species indicates a continuum between isohydric and anisohydric behaviours. Funct. Ecol. 28 (6), 1313–1320. https://doi.org/10.1111/1365-2435.12289.
Kmoch, L., Bou-Lahriss, A., Plieninger, T., 2024. Drought threatens agroforestry landscapes and dryland livelihoods in a north African hotspot of environmental change. Landsc. Urban Plan. 245, 105022. https://doi.org/10.1016/j.landurbplan.2024.105022.
Kobrossi, J., Karam, F., Mitri, G., 2021. Rain pattern analysis using the standardized precipitation index for long-term drought characterization in Lebanon. Arab. J. Geosci. 14 (1), 1–17. https://doi.org/10.1007/s12517-020-06387-3.
Krawczyk, H., Zinke, J., Browne, N., Struck, U., McIlwain, J., O'Leary, M., Garbe-Schönberg, D., 2020. Corals reveal ENSO-driven synchrony of climate impacts on both terrestrial and marine ecosystems in northern Borneo. Sci. Rep. 10 (1), 3678. https://doi.org/10.1038/s41598-020-60525-1.
Krichen, M., Abdalzaher, M.S., Elwekeil, M., Fouda, M.M., 2023. Managing natural disasters: an analysis of technological advancements, opportunities, and challenges. Internet Things Cyber-Phys. Syst. 4, 99–109. https://www.sciencedirect.com/science/article/pii/S2667345223000500.
Kukal, M.S., Irmak, S., 2018. Climate-driven crop yield and yield variability and climate change impacts on the US Great Plains agricultural production. Sci. Rep. 8 (1), 1–18. https://doi.org/10.1038/s41598-018-21848-2.
Kwiatkowski, D., Phillips, P.C., Schmidt, P., Shin, Y., 1992. Testing the null hypothesis of stationarity against the alternative of a unit root: how sure are we that economic time series have a unit root? J. Econ. 54 (1–3), 159–178. https://doi.org/10.1016/0304-4076(92)90104-Y.
Lahaye, S., Curt, T., Fréjaville, T., Sharples, J., Paradis, L., Hély, C., 2018. What are the drivers of dangerous fires in Mediterranean France? Int. J. Wildland Fire 27 (3), 155–163. https://doi.org/10.1071/WF17087.
Latiri, K., Lhomme, J.-P., Annabi, M., Setter, T.L., 2010. Wheat production in Tunisia: Progress, inter-annual variability and relation to rainfall. Eur. J. Agron. 33 (1), 33–42. https://doi.org/10.1016/j.eja.2010.02.004.
Lemenkova, P., 2022. Geomorphology of the Beqaa Valley, Lebanon and Anti-Lebanon Mountains. Acta Scientifica Naturalis 9 (1), 1–22. https://doi.org/10.2478/asn-2022-0002.
Lempereur, M., Limousin, J., Guibal, F., Ourcival, J., Rambal, S., Ruffault, J., Mouillot, F., 2017. Recent climate hiatus revealed dual control by temperature and drought on the stem growth of Mediterranean *Quercus ilex*. Glob. Chang. Biol. 23 (1), 42–55. https://doi.org/10.1111/gcb.13495.
Lempereur, M., Martin-StPaul, N.K., Damesin, C., Joffre, R., Ourcival, J., Rocheteau, A., Rambal, S., 2015. Growth duration is a better predictor of stem increment than carbon supply in a M editerranean oak forest: implications for assessing forest productivity under climate change. New Phytol. 207 (3), 579–590. https://doi.org/10.1111/nph.13400.
Leng, G., Hall, J., 2019. Crop yield sensitivity of global major agricultural countries to droughts and the projected changes in the future. Sci. Total Environ. 654, 811–821. https://doi.org/10.1016/j.scitotenv.2018.10.434.
Lesk, C., Rowhani, P., Ramankutty, N., 2016. Influence of extreme weather disasters on global crop production. Nature 529 (7584), 84–87. https://doi.org/10.1038/nature16467.
Li, J., Wang, Z., Wu, X., Zscheischler, J., Guo, S., Chen, X., 2021. A standardized index for assessing sub-monthly compound dry and hot conditions with application in China. Hydrol. Earth Syst. Sci. 25 (3), 1587–1601. https://doi.org/10.5194/hess-2020-383.

Liu, D., Esquivel-Muelbert, A., Acil, N., Astigarraga, J., Cienciala, E., Fridman, J., Kunstler, G., Matthews, T.J., Ruiz-Benito, P., Sadler, J.P., 2024. Mapping multi-dimensional variability in water stress strategies across temperate forests. Nat. Commun. 15 (1), 8909. https://doi.org/10.1038/s41467-024-53160-1.

Lüdecke, D., Ben-Shachar, M.S., Patil, I., Waggoner, P., Makowski, D., 2021. Performance: an R package for assessment, comparison and testing of statistical models. Journal of Open Source Software 6 (60). https://doi.org/10.21105/joss.03139.

Luković, J., Chiang, J.C.H., Blagojević, D., Sekulić, A., 2021. A later onset of the rainy season in California. Geophys. Res. Lett. 48 (4). https://doi.org/10.1029/2020GL090350 e2020GL090350.

Majdalani, G., 2023. Climat et troubles socio-politiques dans la pyrogéographie Méditerranéenne: Analyse historique et modélisation. Université de Montpellier en cotutelle avec Université Saint-Joseph.

Majdalani, G., Koutsias, N., Faour, G., Adjizian-Gerard, J., Mouillot, F., 2022. Fire regime analysis in Lebanon (2001–2020): combining remote sensing data in a scarcely documented area. Fire 5 (5), 141. https://doi.org/10.3390/fire5050141.

Matiu, M., Ankerst, D.P., Menzel, A., 2017. Interactions between temperature and drought in global and regional crop yield variability during 1961-2014. PLoS One 12 (5), e0178339. https://doi.org/10.1371/journal.pone.0178339.

McDowell, N., Pockman, W.T., Allen, C.D., Breshears, D.D., Cobb, N., Kolb, T., Plaut, J., Sperry, J., West, A., Williams, D.G., Yepez, E.A., 2008. Mechanisms of plant survival and mortality during drought: why do some plants survive while others succumb to drought? New Phytol. 178 (4), 719–739. https://doi.org/10.1111/j.1469-8137.2008.02436.x.

McDowell, N.G., Sapes, G., Pivovaroff, A., Adams, H.D., Allen, C.D., Anderegg, W.R., Arend, M., Breshears, D.D., Brodribb, T., Choat, B., 2022. Mechanisms of woody-plant mortality under rising drought, CO2 and vapour pressure deficit. Nature Reviews Earth & Environment 3 (5), 294–308.

McKee, T.B., Doesken, N.J., Kleist, J., 1993. The relationship of drought frequency and duration to time scales. *Proceedings of the*. In: 8th Conference on Applied Climatology, 17(22), pp. 179–183. https://climate.colostate.edu/pdfs/relationshipofdroughtfrequency.pdf.

Mehrabi, Z., Ramankutty, N., 2019. Synchronized failure of global crop production. Nature Ecology & Evolution 3 (5), 780–786. https://doi.org/10.1038/s41559-019-0862-x.

Mhawej, M., Faour, G., Abdallah, C., Adjizian-Gerard, J., 2016. Towards an establishment of a wildfire risk system in a Mediterranean country. Eco. Inform. 32, 167–184. https://doi.org/10.1016/j.ecoinf.2016.02.003.

Mhawej, M., Faour, G., Adjizian-Gerard, J., 2017. A novel method to identify likely causes of wildfire. Clim. Risk Manag. 16, 120–132. https://doi.org/10.1016/j.crm.2017.01.004.

Muñoz-Sabater, J., Dutra, E., Agustí-Panareda, A., Albergel, C., Arduini, G., Balsamo, G., Boussetta, S., Choulga, M., Harrigan, S., Hersbach, H., 2021. ERA5-land: A state-of-the-art global reanalysis dataset for land applications. Earth System Science Data 13 (9), 4349–4383. https://doi.org/10.5194/essd-13-4349-2021.

Nasrallah, A., Baghdadi, N., El Hajj, M., Darwish, T., Belhouchette, H., Faour, G., Darwich, S., Mhawej, M., 2019. Sentinel-1 data for winter wheat phenology monitoring and mapping. Remote Sens. 11 (19), 2228. https://doi.org/10.3390/rs11192228.

Nasrallah, A., Baghdadi, N., Mhawej, M., Faour, G., Darwish, T., Belhouchette, H., Darwich, S., 2018. A novel approach for mapping wheat areas using high resolution Sentinel-2 images. Sensors 18 (7), 2089. https://doi.org/10.3390/s18072089.

Ndayiragije, J.M., Li, F., 2022. Effectiveness of drought indices in the assessment of different types of droughts, managing and mitigating their effects. Climate 10 (9), 125. https://doi.org/10.3390/cli10090125.

Nogueira, J.M., Rambal, S., Barbosa, J.P.R., Mouillot, F., 2017. Spatial pattern of the seasonal drought/burned area relationship across Brazilian biomes: sensitivity to drought metrics and global remote-sensing fire products. Climate 5 (2), 42. https://doi.org/10.3390/cli5020042.

Páscoa, P., Gouveia, C.M., Russo, A., Trigo, R.M., 2017. The role of drought on wheat yield interannual variability in the Iberian Peninsula from 1929 to 2012. Int. J. Biometeorol. 61, 439–451. https://doi.org/10.1007/s00484-016-1224-x.

Peña-Gallardo, M., Vicente-Serrano, S.M., Domínguez-Castro, F., Beguería, S., 2019. The impact of drought on the productivity of two rainfed crops in Spain. Nat. Hazards Earth Syst. Sci. 19 (6), 1215–1234. https://doi.org/10.5194/nhess-19-1215-2019.

Peña-Gallardo, M., Vicente-Serrano, S.M., Domínguez-Castro, F., Quiring, S., Svoboda, M., Beguería, S., Hannaford, J., 2018. Effectiveness of drought indices in identifying impacts on major crops across the USA. Clim. Res. 75 (3), 221–240. https://doi.org/10.3354/cr01519.

Peters, L.E.R., 2024. The peace imperative for the Sendai framework for disaster risk reduction. Int. J. Disaster Risk Sci. https://doi.org/10.1007/s13753-024-00596-0.

Pook, M., Lisson, S., Risbey, J., Ummenhofer, C.C., McIntosh, P., Rebbeck, M., 2009. The autumn break for cropping in Southeast Australia: trends, synoptic influences and impacts on wheat yield. Int. J. Climatol. 29 (13), 2012–2026. https://doi.org/10.1002/joc.1833.

Proutsos, N., Tigkas, D., 2020. Growth response of endemic black pine trees to meteorological variations and drought episodes in a Mediterranean region. Atmosphere 11 (6), 554.

Reinecke, R., Müller Schmied, H., Trautmann, T., Andersen, L.S., Burek, P., Flörke, M., Gosling, S.N., Grillakis, M., Hanasaki, N., Koutroulis, A., 2021. Uncertainty of simulated groundwater recharge at different global warming levels: A global-scale multi-model ensemble study. Hydrol. Earth Syst. Sci. 25 (2), 787–810. https://doi.org/10.5194/hess-25-787-2021.

Renard, D., Mahaut, L., Noack, F., 2023. Crop diversity buffers the impact of droughts and high temperatures on food production. Environ. Res. Lett. 18 (4), 045002. https://doi.org/10.1088/1748-9326/acc2d6.

Renard, D., Tilman, D., 2019. National food production stabilized by crop diversity. Nature 571 (7764), 257–260. https://doi.org/10.1038/s41586-019-1316-y.

Richardson, D., Black, A.S., Irving, D., Matear, R.J., Monselesan, D.P., Risbey, J.S., Squire, D.T., Tozer, C.R., 2022. Global increase in wildfire potential from compound fire weather and drought. NPJ Climate and Atmospheric Science 5 (1), 23. https://doi.org/10.1038/s41612-022-00248-4.

Ruffault, J., Curt, T., Moron, V., Trigo, R.M., Mouillot, F., Koutsias, N., Pimont, F., Martin-StPaul, N., Barbero, R., Dupuy, J.-L., 2020. Increased likelihood of heat-induced large wildfires in the Mediterranean Basin. Sci. Rep. 10 (1), 13790. https://doi.org/10.1038/s41598-020-70069-z.

Ruffault, J., Martin-StPaul, N., Pimont, F., Dupuy, J.-L., 2018. How well do meteorological drought indices predict live fuel moisture content (LFMC)? An assessment for wildfire research and operations in Mediterranean ecosystems. Agric. For. Meteorol. 262, 391–401. https://doi.org/10.1016/j.agrformet.2018.07.031.

Ruffault, J., Martin-StPaul, N.K., Rambal, S., Mouillot, F., 2013. Differential regional responses in drought length, intensity and timing to recent climate changes in a Mediterranean forested ecosystem. Clim. Chang. 117 (1), 103–117, 0.1007/s10584-012-0559-5.

Sadiqi, S.S.J., Hong, E.-M., Nam, W.-H., Kim, T., 2022. An integrated framework for understanding ecological drought and drought resistance. Sci. Total Environ. 846, 157477. https://doi.org/10.1016/j.scitotenv.2022.157477.

Salehnia, N., Zare, H., Kolsoumi, S., Bannayan, M., 2018. Predictive value of Keetch-Byram drought index for cereal yields in a semi-arid environment. Theor. Appl. Climatol. 134 (3–4), 1005–1014. https://doi.org/10.1007/s00704-017-2315-2.

Salloum, L., Mitri, G., 2014. Assessment of the temporal pattern of fire activity and weather variability in Lebanon. Int. J. Wildland Fire 23 (4), 503–509. https://doi.org/10.1071/WF12101.

Santini, M., Noce, S., Antonelli, M., Caporaso, L., 2022. Complex drought patterns robustly explain global yield loss for major crops. Sci. Rep. 12 (1), 5792. https://doi.org/10.1038/s41598-022-09611-0.

Sattout, E.J., Talhouk, S.N., Caligari, P.D., 2007. Economic value of cedar relics in Lebanon: an application of contingent valuation method for conservation. Ecol. Econ. 61 (2–3), 315–322. https://doi.org/10.1016/j.ecolecon.2006.03.001.

Saxton, K.E., Rawls, W.J., 2006. Soil water characteristic estimates by texture and organic matter for hydrologic solutions. Soil Sci. Soc. Am. J. 70 (5), 1569–1578. https://doi.org/10.2136/sssaj2005.0117.

Schmidt, A.F., Finan, C., 2018. Linear regression and the normality assumption. J. Clin. Epidemiol. 98, 146–151. https://doi.org/10.1016/j.jclinepi.2017.12.006.

Schnabel, F., Liu, X., Kunz, M., Barry, K.E., Bongers, F.J., Bruelheide, H., Fichtner, A., Härdtle, W., Li, S., Pfaff, C.-T., Schmid, B., Schwarz, J.A., Tang, Z., Yang, B., Bauhus, J., Von Oheimb, G., Ma, K., Wirth, C., 2021. Species richness stabilizes productivity via asynchrony and drought-tolerance diversity in a large-scale tree biodiversity experiment. *Science*. Advances 7 (51), eabk1643. https://doi.org/10.1126/sciadv.abk1643.

Seneviratne, S.I., Zhang, X., Adnan, M., Badi, W., Dereczynski, C., Di Luca, A., Ghosh, S., Iskander, I., Kossin, J., Lewis, S., 2021. Weather and climate extreme events in a changing climate (Chapter 11). https://pure.iiasa.ac.at/id/eprint/19093/.

Shaban, A., 2020. Water Resources of Lebanon, vol. 7. Springer International Publishing. https://doi.org/10.1007/978-3-030-48717-1.

Shaban, A., Awad, M., Ghandour, A.J., Telesca, L., 2019. A 32-year aridity analysis: A tool for better understanding on water resources management in Lebanon. Acta Geophys. 67 (4), 1179–1189. https://doi.org/10.1007/s11600-019-00300-7.

Sharma, S., Mujumdar, P., 2017. Increasing frequency and spatial extent of concurrent meteorological droughts and heatwaves in India. Sci. Rep. 7 (1), 15582. https://doi.org/10.1038/s41598-017-15896-3.

Skelton, R.P., West, A.G., Dawson, T.E., 2015. Predicting plant vulnerability to drought in biodiverse regions using functional traits. Proc. Natl. Acad. Sci. 112 (18), 5744–5749. https://doi.org/10.1073/pnas.1503376112.

Slette, I.J., Post, A.K., Awad, M., Even, T., Punzalan, A., Williams, S., Smith, M.D., Knapp, A.K., 2019. How ecologists define drought, and why we should do better. Glob. Chang. Biol. 25 (10), 3193–3200. https://doi.org/10.1111/gcb.14747.

Sun, Y., Robert, C.A., Thakur, M.P., 2024. Drought intensity and duration effects on morphological root traits vary across trait type and plant functional groups: A meta-analysis. BMC Ecology and Evolution 24 (1), 92. https://doi.org/10.1186/s12862-024-02275-6.

Swain, D.L., 2021. A shorter, sharper rainy season amplifies California wildfire risk. Geophys. Res. Lett. 48 (5). https://doi.org/10.1029/2021GL092843 e2021GL092843.

Tigkas, D., Tsakiris, G., 2015. Early estimation of drought impacts on Rainfed wheat yield in Mediterranean climate. Environ. Process. 2 (1), 97–114. https://doi.org/10.1007/s40710-014-0052-4.

Touchan, R., Anchukaitis, K.J., Shishov, V.V., Sivrikaya, F., Attieh, J., Ketmen, M., Stephan, J., Mitsopoulos, I., Christou, A., Meko, D.M., 2014. Spatial patterns of eastern Mediterranean climate influence on tree growth. The Holocene 24 (4), 381–392. https://doi.org/10.1177/0959683613518594.

Touchan, R., Xoplaki, E., Funkhouser, G., Luterbacher, J., Hughes, M.K., Erkan, N., Akkemik, Ü., Stephan, J., 2005. Reconstructions of spring/summer precipitation for the eastern Mediterranean from tree-ring widths and its connection to large-scale atmospheric circulation. Clim. Dyn. 25, 75–98. https://doi.org/10.1007/s00382-005-0016-5.

Trabelsi, L., Gargouri, K., Ayadi, M., Mbadra, C., Ben Nasr, M., Ben Mbarek, H., Ghrab, M., Ben Ahmed, G., Kammoun, Y., Loukil, E., Maktouf, S., Khlifi, M., Gargouri, R., 2022. Impact of drought and salinity on olive potential yield, oil and

fruit qualities (cv. Chemlali) in an arid climate. Agric. Water Manag. 269, 107726. https://doi.org/10.1016/j.agwat.2022.107726.
Tramblay, Y., Koutroulis, A., Samaniego, L., Vicente-Serrano, S.M., Volaire, F., Boone, A., Le Page, M., Llasat, M.C., Albergel, C., Burak, S., 2020. Challenges for drought assessment in the Mediterranean region under future climate scenarios. Earth Sci. Rev. 210, 103348.
Tranmer, M., Elliot, M., 2008. Multiple linear regression. The Cathie Marsh Centre for Census and Survey Research (CCSR) 5 (5), 1–5.
Turco, M., Jerez, S., Augusto, S., Tarín-Carrasco, P., Ratola, N., Jiménez-Guerrero, P., Trigo, R.M., 2019. Climate drivers of the 2017 devastating fires in Portugal. Sci. Rep. 9 (1), 13886. https://doi.org/10.1038/s41598-019-50281-2.
Turco, M., von Hardenberg, J., AghaKouchak, A., Llasat, M.C., Provenzale, A., Trigo, R. M., 2017. On the key role of droughts in the dynamics of summer fires in Mediterranean Europe. Sci. Rep. 7 (1), 81. https://doi.org/10.1038/s41598-017-00116-9.
UNDRR. (2015, June 29). Sendai Framework for Disaster Risk Reduction 2015–2030 | UNDRR. https://www.undrr.org/publication/sendai-framework-disaster-risk-reduction-2015-2030.
Urbieta, I.R., Zavala, G., Bedia, J., Gutiérrez, J.M., San Miguel-Ayanz, J., Camia, A., Keeley, J.E., Moreno, J.M., 2015. Fire activity as a function of fire–weather seasonal severity and antecedent climate across spatial scales in southern Europe and Pacific western USA. Environ. Res. Lett. 10 (11), 114013. https://doi.org/10.1088/1748-9326/10/11/114013.
Vagnon, C., Olden, J.D., Boulêtreau, S., Bruel, R., Chevalier, M., Garcia, F., Holtgrieve, G., Jackson, M., Thebault, E., Tedesco, P.A., 2024. Ecosystem synchrony: an emerging property to elucidate ecosystem responses to global change. Trends Ecol. Evol. https://doi.org/10.1016/j.tree.2024.08.003.
Valencia, E., De Bello, F., Galland, T., Adler, P.B., Lepš, J., E-Vojtkó, A., Van Klink, R., Carmona, C. P., Danihelka, J., Dengler, J., Eldridge, D. J., Estiarte, M., García-González, R., Garnier, E., Gómez-García, D., Harrison, S. P., Herben, T., Ibáñez, R., Jentsch, A., … Götzenberger, L., 2020. Synchrony matters more than species richness in plant community stability at a global scale. Proc. Natl. Acad. Sci. 117 (39), 24345–24351. https://doi.org/10.1073/pnas.1920405117.
Verner, D., Ashwill, M., Christensen, J., Mcdonnell, R., Redwood, J., Jomaa, I., Saade, M., Massad, R., Chehade, A., Bitar, A., 2018. Droughts and Agriculture in Lebanon.
Verran, J.A., Ferketich, S.L., 1987. Testing linear model assumptions: residual analysis. Nurs. Res. 36 (2), 127–129.
Vicente-Serrano, S.M., Beguería, S., López-Moreno, J.I., 2010. A multiscalar drought index sensitive to global warming: the standardized precipitation evapotranspiration index. J. Clim. 23 (7), 1696–1718. https://doi.org/10.1175/2009JCLI2909.1.
Vicente-Serrano, S.M., Beguería, S., Lorenzo-Lacruz, J., Camarero, J.J., López-Moreno, J. I., Azorin-Molina, C., Revuelto, J., Morán-Tejeda, E., Sanchez-Lorenzo, A., 2012. Performance of drought indices for ecological, agricultural, and hydrological applications. Earth Interact. 16 (10), 1–27. https://doi.org/10.1175/2012EI000434.1.
Vicente-Serrano, S.M., Quiring, S.M., Peña-Gallardo, M., Yuan, S., Domínguez-Castro, F., 2020. A review of environmental droughts: increased risk under global warming? Earth Sci. Rev. 201, 102953.
Vissio, G., Turco, M., Provenzale, A., 2023. Testing drought indicators for summer burned area prediction in Italy. Nat. Hazards 116 (1), 1125–1137. https://doi.org/10.1007/s11069-022-05714-z.
von Matt, C.N., Muelchi, R., Gudmundsson, L., Martius, O., 2024. Compound droughts under climate change in Switzerland. Natural Hazards and Earth System Sciences Discussions 2024, 1–37. https://doi.org/10.5194/nhess-24-1975-2024.
Wang, H., Vicente-Serrano, S.M., Tao, F., Zhang, X., Wang, P., Zhang, C., Chen, Y., Zhu, D., El Kenawy, A., 2016. Monitoring winter wheat drought threat in northern China using multiple climate-based drought indices and soil moisture during 2000–2013. Agric. For. Meteorol. 228, 1–12. https://doi.org/10.1016/j.agrformet.2016.06.004.
Wei, T., Simko, V. R., Levy, M., Xie, Y., Jin, Y., & Zemla, J. (2021). Package "corrplot": visualization of a correlation matrix. 2017. Version 0.84.
Westerling, A.L., Hidalgo, H.G., Cayan, D.R., Swetnam, T.W., 2006. Warming and earlier spring increase Western U.S. Forest wildfire activity. Science 313 (5789), 940–943. https://doi.org/10.1126/science.1128834.
Wickham, H., Chang, W., & Wickham, M. H. (2016). Package 'ggplot2.' *Create Elegant Data Visualisations Using the Grammar of Graphics.* Version, 2(1), 1–189.
Wilhite, D., & Pulwarty, R. S. (2017). Drought and water crises: integrating science, management, and policy. CRC Press. https://books.google.com/books?hl=fr&lr=&id=ADoPEAAAQBAJ&oi=fnd&pg=PP1&dq=81.%09Wilhite,+D.,+%26+Pulwarty,+R.+S.+(Eds.).+(2017).+Drought+and+water+crises:+integrating+science,+management,+and+policy.+CRC+Press.&ots=wz99L7F5bS&sig=9m4p5HG0UfPs6N3mt8JjqdPsTfg.
Wilhite, D.A., Glantz, M.H., 1985. Understanding: the drought phenomenon: the role of definitions. Water Int. 10 (3), 111–120. https://doi.org/10.1080/02508068508686328.
Wu, J., Yao, H., Chen, X., Wang, G., Bai, X., Zhang, D., 2022. A framework for assessing compound drought events from a drought propagation perspective. J. Hydrol. 604, 127228. https://doi.org/10.1016/j.jhydrol.2021.127228.
Xing, Z., Ma, M., Wei, Y., Zhang, X., Yu, Z., Yi, P., 2020. A new agricultural drought index considering the irrigation water demand and water supply availability. Nat. Hazards 104 (3), 2409–2429. https://doi.org/10.1007/s11069-020-04278-0.
Xue, R., Sun, B., Li, W., Li, H., Zhou, B., 2024. Future changes in compound drought events and associated population and GDP exposure in China based on CMIP6. Atmospheric and Oceanic Science Letters 17 (3), 100461. https://doi.org/10.1016/j.aosl.2024.100461.
Yang, C., Fraga, H., van Ieperen, W., Santos, J.A., 2020. Assessing the impacts of recent-past climatic constraints on potential wheat yield and adaptation options under Mediterranean climate in southern Portugal. Agric. Syst. 182, 102844.
Yihdego, Y., Vaheddoost, B., Al-Weshah, R.A., 2019. Drought indices and indicators revisited. Arab. J. Geosci. 12 (3), 69. https://doi.org/10.1007/s12517-019-4237-z.
Yu, H., Zhang, Q., Sun, P., Song, C., 2018. Impact of droughts on winter wheat yield in different growth stages during 2001–2016 in eastern China. Int. J. Disaster Risk Sci. 9 (3), 376–391. https://doi.org/10.1007/s13753-018-0187-4.
Zang, C.S., Buras, A., Esquivel-Muelbert, A., Jump, A.S., Rigling, A., Rammig, A., 2020. Standardized drought indices in ecological research: why one size does not fit all. Glob. Chang. Biol. 26 (2), 322–324. https://doi.org/10.1111/gcb.14809.
Zargar, A., Sadiq, R., Naser, B., Khan, F.I., 2011. A review of drought indices. Environ. Rev. 19 (NA), 333–349. https://doi.org/10.1139/a11-013.
Zeileis, A., Hothorn, T., 2002. Diagnostic checking in regression relationships. https://journal.r-project.org/articles/RN-2002-018/RN-2002-018.pdf.
Zhou, H., Zhou, W., Liu, Y., Yuan, Y., Huang, J., Liu, Y., 2020. Identifying spatial extent of meteorological droughts: an examination over a humid region. J. Hydrol. 591, 125505. https://doi.org/10.1016/j.jhydrol.2020.125505.
Zribi, L., Mouillot, F., Guibal, F., Rejeb, S., Rejeb, M.N., Gharbi, F., 2016. Deep soil conditions make Mediterranean cork oak stem growth vulnerable to autumnal rainfall decline in Tunisia. Forests 7 (10), 245. https://doi.org/10.3390/f7100245.